Article

Circadian plasticity evolves through regulatory changes in a neuropeptide gene

https://doi.org/10.1038/s41586-024-08056-x

Received: 5 July 2023

Accepted: 16 September 2024

Published online: 16 October 2024

Open access

Check for updates

Michael P. Shahandeh[1,3]✉, Liliane Abuin[1], Lou Lescuyer De Decker[1], Julien Cergneux[1], Rafael Koch[2], Emi Nagoshi[2] & Richard Benton[1]✉

Many organisms, including cosmopolitan drosophilids, show circadian plasticity, varying their activity with changing dawn–dusk intervals[1]. How this behaviour evolves is unclear. Here we compare *Drosophila melanogaster* with *Drosophila sechellia*, an equatorial, ecological specialist that experiences minimal photoperiod variation, to investigate the mechanistic basis of circadian plasticity evolution[2]. *D. sechellia* has lost the ability to delay its evening activity peak time under long photoperiods. Screening of circadian mutants in *D. melanogaster*/*D. sechellia* hybrids identifies a contribution of the neuropeptide pigment-dispersing factor (Pdf) to this loss. *Pdf* exhibits species-specific temporal expression, due in part to *cis*-regulatory divergence. RNA interference and rescue experiments in *D. melanogaster* using species-specific *Pdf* regulatory sequences demonstrate that modulation of this neuropeptide's expression affects the degree of behavioural plasticity. The *Pdf* regulatory region exhibits signals of selection in *D. sechellia* and across populations of *D. melanogaster* from different latitudes. We provide evidence that plasticity confers a selective advantage for *D. melanogaster* at elevated latitude, whereas *D. sechellia* probably suffers fitness costs through reduced copulation success outside its range. Our findings highlight this neuropeptide gene as a hotspot locus for circadian plasticity evolution that might have contributed to both *D. melanogaster*'s global distribution and *D. sechellia*'s specialization.

Nervous systems coordinate animals' behavioural responses to the external world. This task becomes challenging when environments are variable, particularly for broadly distributed species. One way to face changing conditions is with behavioural plasticity—that is, the ability to adjust behavioural phenotypes to match environmental fluctuations. Many examples of plastic behaviours exist: songbirds shift their vocalization frequencies in response to anthropogenic noise[3], and lizards change their basking behaviour according to altitude[4]. How behavioural plasticity is determined and evolves is unknown.

A common example of plastic behaviour is circadian activity, whereby species adjust their activity patterns in response to seasonal variation in day length[5]. This ability is critical, because circadian activity coordinates specific behaviours with optimal activity throughout the day to maximize food availability and synchronize social behaviours[6]. Deviations from regular circadian patterns can negatively affect fitness and species persistence[7]. Drosophilids are a powerful system with which to study circadian behavioural plasticity. These flies show bouts of activity surrounding dawn and dusk (morning and evening activity peaks), separated by a period of relative inactivity[8]. The best-studied species, the cosmopolitan *Drosophila melanogaster*, plasticly adjusts its circadian rhythm depending on seasonal variation in photoperiod[1]. Notably, the degree of photoperiod plasticity of different strains of this species correlates with their latitude of origin[9]. Moreover, several distantly related, high-latitude species have evolved divergent patterns of activity and extreme plasticity, allowing their daily activity to match long summer days[10].

An interesting comparison species to *D. melanogaster* is the closely related *Drosophila sechellia*[2] (Fig. 1a), which is endemic to the equatorial Seychelles islands, where it experiences little seasonal photoperiod variation (Fig. 1a,b). Here we describe marked differences in the circadian activity and plasticity of *D. sechellia* and *D. melanogaster*, and investigate the mechanistic basis of these differences.

Species-specific evening peak plasticity

We first measured the circadian behaviour of *D. melanogaster* and *D. sechellia* under a 12:12 h light:dark cycle (12:12 h LD) and four extended photoperiods, ranging from mild (14:10 h LD) to extreme (20:4 h LD) (Fig. 1c). We used males of two strains each of *D. melanogaster* and *D. sechellia* (Supplementary Table 1), to distinguish inter- from intraspecific differences. The *D. melanogaster* strains (*Dmel*CS and *Dmel*OR) were collected at around 41° N and 44° N, respectively; the *D. sechellia* strains (*Dsec*07 and *Dsec*28) were from the Seychelles, around 4° S (Fig. 1a). The *D. melanogaster* and *D. sechellia* strains thus initially evolved in environments with annual photoperiod variation on the scale of several hours or minutes, respectively (Fig. 1b). Under

[1]Center for Integrative Genomics, Faculty of Biology and Medicine, University of Lausanne, Lausanne, Switzerland. [2]Department of Genetics and Evolution & Institute of Genetics and Genomics of Geneva (iGE3), University of Geneva, Geneva, Switzerland. [3]Present address: Department of Biology, Hofstra University, Hempstead, NY, USA. ✉e-mail: Michael.P.Shahandeh@hofstra.edu; Richard.Benton@unil.ch

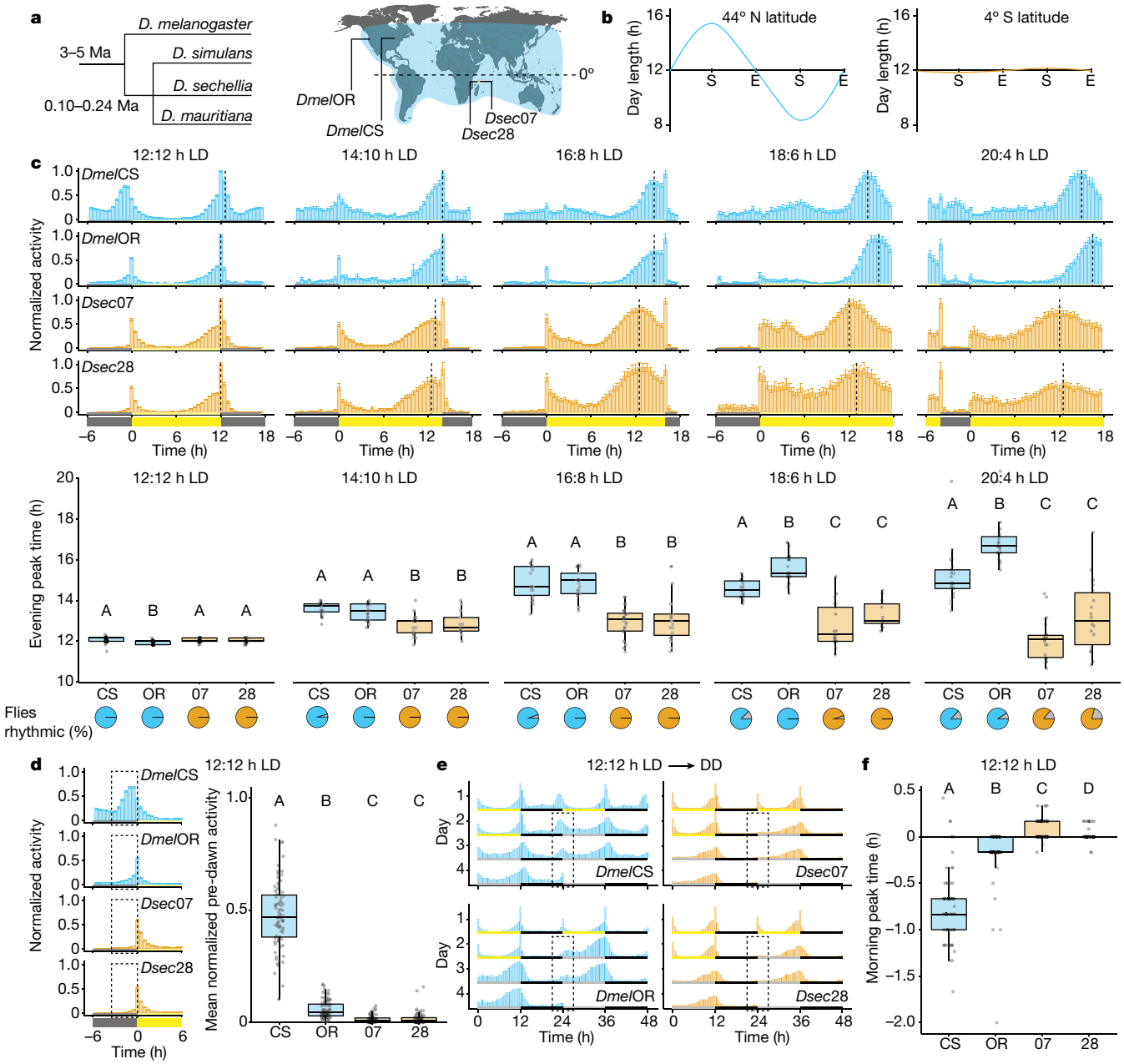

Fig. 1 | Interspecific circadian differences in *D. sechellia* and *D. melanogaster*. **a**, *D. melanogaster* (*Dmel*) subgroup phylogeny (left) and ranges (right) of *Dmel* (blue) and *D. sechellia* (*Dsec*) (orange), with approximate collection sites of strains. **b**, Approximate photoperiod variation (www.srrb.noaa.gov) at collection sites of *Dmel* (left) and *Dsec* (right) strains. **c**, Top, mean normalized activity of *Dmel* and *Dsec* under the indicated photoperiods. Yellow and grey bars indicate lights-on and lights-off, respectively; vertical dashed lines indicate average timing of the evening peak; error bars represent s.e.m. Middle, box plots (Methods) depicting evening peak time for individual flies under each photoperiod. Bottom, pie charts representing the proportion of flies that maintained rhythmic behaviour (colour) or no significant periodicity (grey). *n*, 12:12 h LD: CS (18), OR (21), 07 (24), 28 (19); 14:10 h LD: CS (22), OR (22), 07 (19), 28 (13); 16:8 h LD: CS (18), OR (21), 07 (24), 28 (19); 18:6 h LD: CS (22), OR (23), 07 (21), 28 (11); 20:4 h LD: CS (21), OR (22), 07 (19), 28 (18). **d**, Left, mean normalized activity of *Dmel* and *Dsec* under 12:12 h LD during the morning activity peak (−6 to +6 h data from **c**). Dashed boxes highlight the predawn period. Right, mean normalized activity of individual flies within the predawn period. *n*: CS (89), OR (93), 07 (95), 28 (91). **e**, Double-plotted actograms depicting the transition from the last 2 days of 12:12 h LD to DD for each strain. Dashed boxes highlight morning activity peak period during DD, −3 to +3 h. *n*: CS (29), OR (32), 07 (29), 28 (22). Grey bars indicate timing of subjective lights-on during DD. **f**, Morning peak time, from lights-on, for flies from **d**. **c**,**d**,**f**, Letters A–D indicate significant differences, $P < 0.05$ (pairwise Wilcoxon test with Bonferroni correction). E, equinox; S, solstice.

each photoperiod, all strains showed activity peaks during the morning and evening, although the timing of peak evening activity varied by photoperiod (Fig. 1c). We quantified the average evening peak time of the last 4 of 7 days in a given photoperiod (Methods and Fig. 1c). For *D. melanogaster*, the timing of the evening activity peak was commensurately delayed as photoperiod increased (Fig. 1c and Extended Data Fig. 1a). By contrast, for *D. sechellia* we observed notably little evening peak plasticity, with a median delay in evening peak time of maximum around 1 h regardless of photoperiod (Fig. 1c and Extended Data Fig. 1a). Importantly, we detected a significant interaction between photoperiod and species (Extended Data Fig. 1a). Under the most extreme photoperiod, many *D. sechellia* showed arrhythmicity (Fig. 1c) and decreased activity (Extended Data Fig. 1b), contributing to the increased variability in evening peak time. The absence of evening

peak plasticity was also apparent in female *D. sechellia* (Extended Data Fig. 1c).

Species-specific morning peak activity

D. sechellia is much less active during the dark phase than *D. melanogaster* (Fig. 1c). Quantification of predawn activity (3 h preceding lights-on) under 12:12 h LD showed that *D. sechellia* was generally inactive during this period, whereas *D. melanogaster* showed ample, albeit strain-specific, activity (Fig. 1d), a difference also seen in females (Extended Data Fig. 1d). We next measured free-running activity by acclimating our strains to 12:12 h LD before submitting them to constant dark conditions (DD). Both *D. melanogaster* and *D. sechellia* remained rhythmic under DD (Fig. 1e) showing a period of around 24 h (Extended Data Fig. 1e,f). However, at the subjective dawn, *D. melanogaster* showed clear activity peaks, whereas *D. sechellia* exhibited very little activity, even during the first day of DD (Fig. 1e). Low predawn activity therefore reflects a reduced morning activity peak of *D. sechellia*, and the activity observed after lights-on under 12:12 h LD is probably largely a startle response. Consistently, when we quantified morning peak timing under 12:12 h LD, *D. melanogaster* reached peak activity before lights-on, as previously described[11], whereas *D. sechellia* peaked only at, or just after, lights-on (Fig. 1f).

D. sechellia-specific loss of plasticity

We extended our analyses to two other *D. melanogaster* strains[12] (collected near their ancestral range[13] (roughly 16° S)), two additional *D. sechellia* strains, as well as closer relatives of *D. sechellia* (Fig. 1a): *Drosophila simulans*[12] (collected from its ancestral range[14], around 19° S) and *Drosophila mauritiana* (endemic to Mauritius, roughly 20° S) (Extended Data Fig. 2a,d). Under 16:8 h LD conditions, all *D. melanogaster*, *D. simulans* and *D. mauritiana* strains exhibited a higher degree of evening peak plasticity compared with *D. sechellia* (Extended Data Fig. 2b). The degree of evening peak plasticity reflected a latitudinal effect: tropical *D. melanogaster* strains showed reduced plasticity when compared with high-latitude strains (Extended Data Fig. 2b). The majority of non-*D. sechellia* strains also exhibited substantial morning activity (Extended Data Fig. 2c). These results indicate that the lack of plasticity and reduction in morning activity observed in *D. sechellia* probably represent losses in this lineage.

Pdf underlies species plasticity loss

To identify the genetic basis of species differences, we took a candidate approach. In *D. melanogaster*, 150 circadian neurons contain a molecular feedback loop that tracks a period of approximately 24 h (refs. 15,16) and controls the rhythmic expression of effectors, representing many candidates (Fig. 2a). Because *D. sechellia* traits reflect evolutionary losses, we reasoned that causal *D. sechellia* alleles were probably recessive to *D. melanogaster* and thus designed a screen in *D. melanogaster*/*D. sechellia* hybrids (Fig. 2b). We generated hemizygous test hybrids containing *D. melanogaster* mutations for individual candidates to show any recessive phenotype of the *D. sechellia* allele at the same locus. We also generated heterozygous control hybrids, using either the *D. melanogaster* w^{1118} strain (a common genetic background of mutants) or CS^{W} (*pigment-dispersing factor* (*Pdf*); Methods) and each *D. sechellia* strain. Differences between control and test hybrids are probably due to loss of the *D. melanogaster* allele in the test hybrid. Gene dosage effects were assessed by testing control *D. melanogaster* hemizygotes. Genes whose mutations showed a consistent effect in both test hybrid backgrounds compared with control hybrids, but not in hemizygous *D. melanogaster*, were considered the strongest candidates to explain interspecific differences (Fig. 2c).

To assess candidates for an effect on evening peak plasticity, we observed test and control hybrids under 16:8 h LD. Control hybrids of either the w^{1118} (Extended Data Fig. 3a–d) or CS^{W} background (Fig. 2d,e and Extended Data Fig. 4) showed a higher degree of evening peak plasticity than their *D. sechellia* parental strain, confirming that the *D. melanogaster* genotype underlying plasticity is partially dominant to that of *D. sechellia*, although the degree of plasticity is strain dependent. We screened 14 genes representing the majority of the circadian feedback loop, and many of its modulators and effectors. Mutations in only one reduced evening peak plasticity in both test hybrid backgrounds but not in hemizygous *D. melanogaster*: *Pdf* (Fig. 2d,e and Extended Data Fig. 3e–g). This is a promising gene in regard to explaining species differences because, in *D. melanogaster*, Pdf is essential for delaying the phase of the endogenous clock in circadian neurons under long photoperiods[17–19].

Many genes affect morning activity

We also screened these genotypes under 12:12 h LD and quantified predawn activity as a measure of morning activity (Extended Data Fig. 5a–d). w^{1118} control hybrids showed intermediate morning activity relative to parental strains. Consistently, four genes showed an effect in test hybrids of both backgrounds (Fig. 2f,g) but not in hemizygous *D. melanogaster* (Extended Data Fig. 5e–g). These encode the transcriptional feedback loop proteins CYC and CRY (responsible for light-dependent synchronization of the molecular clock[20]), and Hr38 and VRI, which are neural activity-dependent transcriptional and post-transcriptional regulators of *Pdf*, respectively[21,22] (Fig. 2h).

Species-specific *Pdf* expression

We focused on *Pdf*, because of its unique effect on evening peak plasticity and evidence that *trans*-regulation of *Pdf* expression influences morning peak activity. The *Pdf* coding sequence is almost perfectly conserved across species (Extended Data Fig. 6), indicating that behavioural divergence must be due to species-specific differences in *Pdf* expression. In *D. melanogaster*, Pdf is expressed in eight neurons in each brain hemisphere: four large and four small ventrolateral clock neurons (l-LNvs and s-LNvs, respectively) (Fig. 3a). s-LNvs control the timing of morning activity, whereas l-LNvs can delay the phase of the evening activity peak under long photoperiods[23–26], although a functional clock is required in both for photoperiod plasticity[24,27]. The spatial distribution of this neuropeptide is conserved in *D. sechellia* (Fig. 3a), consistent with analysis across diverse drosophilids[28], suggesting that species-specific differences exist in the temporal pattern and/or levels of Pdf expression.

Using quantitative single-molecule RNA fluorescence in situ hybridization (smFISH), we compared *Pdf* transcript levels between *D. melanogaster* and *D. sechellia*, focusing primarily on s-LNvs, in which Pdf expression shows a clear temporal pattern that more probably correlates with secretion of this neuropeptide[29]. Under 12:12 h LD, *Dmel*CS expressed overall more *Pdf* RNA than *Dsec*07 throughout the morning activity peak, particularly predawn, with *Dsec*07 reaching near-similar levels only after lights-on (Fig. 3b). Immunofluorescence quantification of Pdf peptide levels in the axonal projections of s-LNvs for the same time points spanning the morning activity peak (Fig. 3c) showed a consistently high level of Pdf in *D. melanogaster*, including in the hours preceding lights-on. By contrast, in *D. sechellia*, Pdf signal was lower in the predawn period and increased to an equivalent amount to *D. melanogaster* only by lights-on. This pattern corresponds well to that of the relative levels of *Pdf* transcripts, and to species differences in morning peak activity at these times (Fig. 1c,d). We also analysed Pdf immunofluorescence in the s-LNv soma. Consistent with previous observations[29], Pdf signal remained high across the morning peak times in the s-LNv soma of *D. melanogaster* (Fig. 3d). In *D. sechellia*, the Pdf

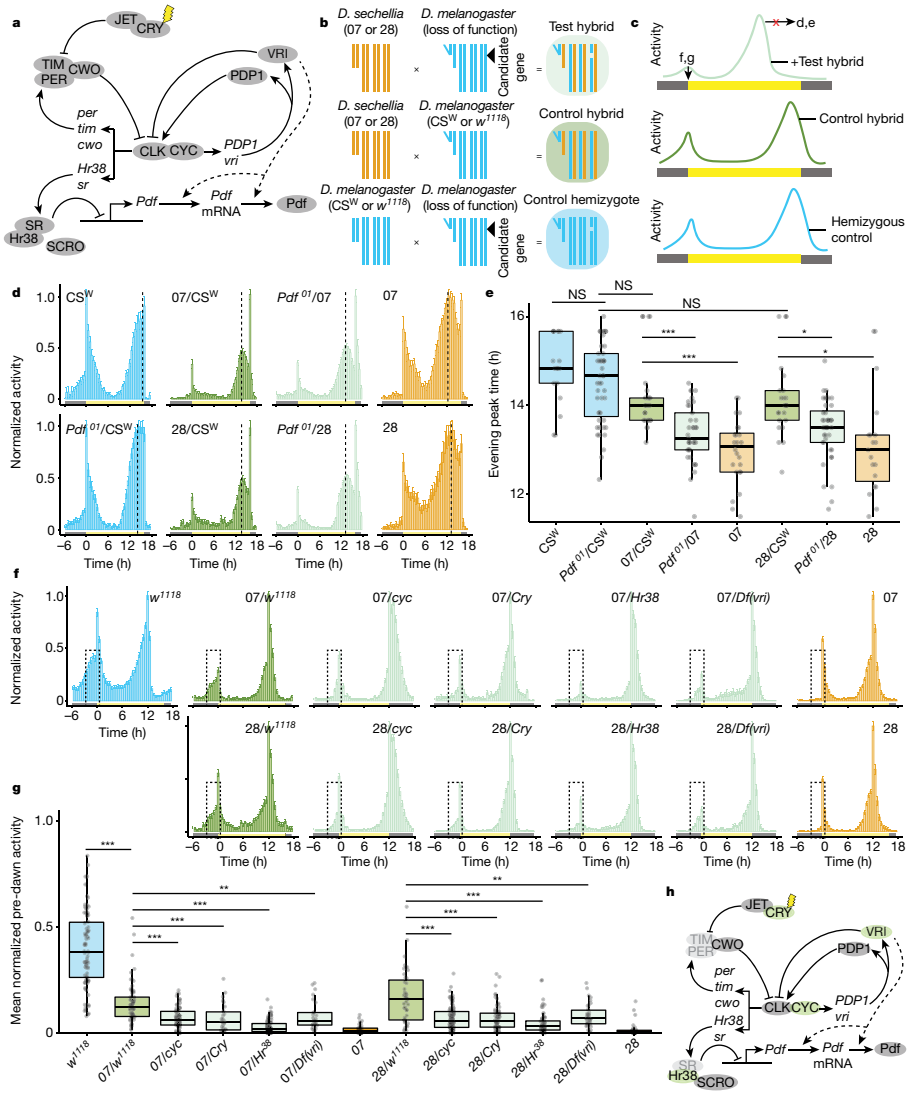

Fig. 2 | Genetic screens for interspecific circadian differences. a, The *D. melanogaster* circadian clock. Arrows denote transcriptional activation, blunt-ended connectors represent repression/degradation and dashed lines indicate hypothesized connections. **b**, Crossing schemes of the genetic screen. The fourth chromosome is not shown. **c**, Schematics illustrating the sought-after behavioural phenotypes of hybrid genotypes. **d**, Mean normalized activity of the indicated genotypes under 16:8 h LD. *n*: CS^W (16), Pdf^{01}/CS^W (47), $07/CS^W$ (25), $28/CS^W$ (23), $07/Pdf^{01}$ (37), $28/Pdf^{01}$ (40), 07 (24), 28 (19). Full screen results are given in Extended Data Fig. 3. **e**, Evening peak time for the flies depicted in **d**. $^*P < 0.05$, $^{***}P < 0.001$ (Wilcoxon tests with Bonferroni correction). Comparisons were made only between control and test hybrids of the same genetic backgrounds. **f**, Mean normalized activity of the indicated genotypes under 12:12 h LD, illustrating the mutations showing reduced morning activity in test hybrids. Dashed boxes highlight the predawn area used to quantify predawn activity, 3 h before lights-on. Error bars represent s.e.m. Full screen results are shown in Extended Data Fig. 5. **g**, Mean normalized predawn activity for the genotypes shown in **f**. $^{**}P < 0.01$, $^{***}P < 0.001$ (Wilcoxon tests comparing each test hybrid with the appropriate control hybrid strain, with Bonferroni correction). **h**, The circadian molecular network, in which screen hits for morning activity are highlighted in green; genes depicted in light grey could not be tested (Methods). mRNA, messenger RNA; NS, not significantly different.

signal began high but dropped significantly only after lights-on. These observations suggest that *D. sechellia* has a weaker and/or shorter pulse of *Pdf* expression in s-LNvs around the morning peak compared with *D. melanogaster*, such that once this neuropeptide accumulates to high levels in the axon termini at or after lights-on (Fig. 3c), it becomes depleted from the soma (Fig. 3d).

Pdf expression in the l-LNvs of *D. melanogaster* has been described as high and constant[29]. Consistently, using smFISH under both 12:12 and 16:8 h LD, we observed relatively stable expression across time points (Extended Data Fig. 7a,b). However, we noted a *D. melanogaster*-specific drop in transcript abundance under 12:12 h LD following lights-off that was not apparent under 16:8 h LD, when the lights remained on at the same time point. Pdf immunofluorescence intensity in the l-LNv soma was not significantly different between these species under both photoperiods, but showed substantial variability, particularly for *D. sechellia* under 16:8 h LD (Extended Data Fig. 7c,d). It remains unclear whether and how Pdf secretion rate in the l-LNv axon termini differs between these species under distinct photoperiods.

Pdf neuron structural plasticity

In *D. melanogaster*, the axonal projections of s-LNvs to the dorsal circadian neurons (Fig. 3a) show circadian structural plasticity, reaching peak branching complexity during the day[30]. This phenomenon depends, in part, on cyclic expression and release of Pdf from both s-LNvs and l-LNvs and expression of the Pdf receptor[31]. To test whether the species-specific temporal patterns of Pdf expression are accompanied by differences in neuronal remodelling, we quantified the

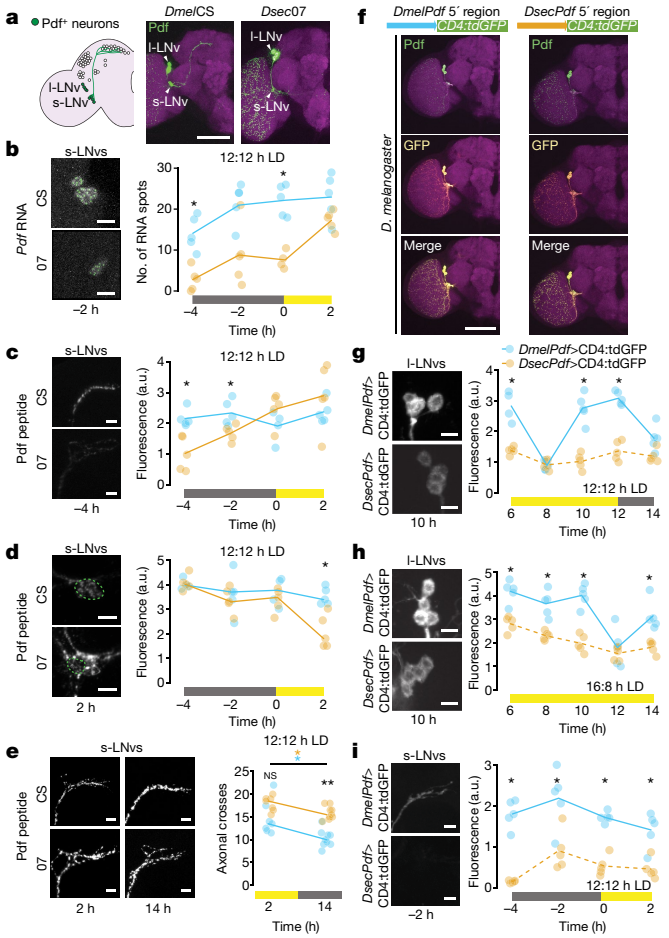

Fig. 3 | Species-specific *cis*-regulatory elements affect *Pdf* expression. **a**, Schematic of the *D. melanogaster* circadian clock neuron network. Pdf-positive s-LNvs and l-LNvs are highlighted. Immunofluorescence for Pdf (green) and cadherin-N (magenta) on brains of the indicated strains at 2 h under 12:12 h LD. **b**–**d**, Left, representative images of *Pdf* smFISH (**b**) and Pdf immunofluorescence (**c**,**d**) in s-LNv soma (**b**,**d**) and axon termini (**c**) for strains under 12:12 h LD at the indicated time points. Right, quantifications of each strain at four time points spanning the predawn period. **e**, Left, Pdf immunofluorescence in s-LNv axon termini for indicated strains during the day (2 h) and night (14 h) under 12:12 h LD. Right, quantifications of axonal branching complexity using Scholl analysis. *n*: CS 2 h (7), 07 2 h (7), CS 14 h (9), 07 14 h (9). **f**, Top, schematic illustrating *Pdf* transcriptional reporters. Bottom, immunofluorescence for Pdf (green), GFP (yellow) and cadherin-N (magenta) in brains of *D. melanogaster* (at 2 h) expressing species-specific *Pdf* reporters. **g**–**i**, Left, representative images of GFP immunofluorescence in l-LNvs (**g**,**h**) and s-LNv axonal projections (**i**) for *Dmel* and *DsecPdf* 5′-regulatory reporter strains under 12:12 h LD (**g**,**i**) and 16:8 h LD (**h**) at the indicated time points. Right, quantifications at time points spanning the evening activity peak period (**g**,**h**) and predawn period (**i**). Although signals are weak in some *Dsec* images, the structures were readily identified in thresholded images. **b**–**e**,**g**–**i**, Plotted values are the average of both hemispheres; lines connect medians of time points within genotypes. *$P < 0.05$, **$P < 0.01$ (Wilcoxon tests with Bonferroni correction). Scale bars, 100 µm (**a**,**f**), 10 µm (**b**–**e**,**g**–**i**). **b**–**d**,**g**–**i**, $n = 5$ brains per strain per time point. a.u., arbitrary units.

branching complexity of s-LNv projections during both light (2 h) and dark (14 h) phases under 12:12 h LD (Fig. 3e). During the light phase, we found statistically indistinguishable levels of complexity in the two species and observed in both a decrease in complexity from the light to the dark phase. However, branching complexity in the dark phase was significantly lower in *D. melanogaster* than in *D. sechellia* (Fig. 3e). This apparent lower structural plasticity of *D. sechellia* Pdf neurons corroborates the reduced dynamic changes in Pdf expression in this species.

Cis-regulatory evolution of *Pdf*

Because our hybrid screen identified an effect of the *Pdf* locus (and not a *trans*-regulator) on evening peak delay, we hypothesized that expression differences result from divergence in this gene's *cis*-regulatory region. We cloned around 2.4 kb genomic DNA 5′ of *Pdf* from *D. melanogaster* (similar to the sequence used in ref. 29) and *D. sechellia* upstream of a green fluorescent protein (GFP) reporter. These constructs were integrated in an identical location in *D. melanogaster*, facilitating comparison of their activity in a common genomic and *trans* environment. Both species' *Pdf* reporters exclusively labelled the l-LNvs and s-LNvs (Fig. 3f). We first measured reporter expression in l-LNvs, focusing on behaviourally relevant time points under 12:12 and 16:8 h LD (Fig. 3g,h). In l-LNvs, throughout the evening activity peak under both photoperiods, the *D. sechellia* 5′-regulatory region consistently drove lower and more constant reporter expression relative to the *D. melanogaster* sequence (Fig. 3g,h). Notably, the *D. melanogaster Pdf* reporter showed a sudden drop in expression at either 8 h (under 12:12 h LD) or 12 h (under 16:8 h LD), before returning to a higher level; this expression pattern potentially reflects a new pulse in transcriptional activity that is photoperiod sensitive.

In *D. melanogaster*, s-LNvs are essential for resetting the phase of the circadian clock[32,33] and morning peak activity[23,25]. We therefore compared reporter expression in s-LNv axonal projections—in which the highest cyclic Pdf expression was observed over a 24 h period[29]—for time points spanning the morning activity peak (Fig. 3i). The *D. sechellia* 5′-regulatory sequence drives lower expression of the reporter but, in contrast to reporter expression in l-LNvs during the evening peak, with a similar temporal pattern.

These results indicate divergence of the *Pdf* 5′-regulatory region between *D. sechellia* and *D. melanogaster*, most probably affecting transcriptional activity. However, because the region encompasses the *Pdf* 5′-untranslated region, we cannot exclude the possibility that it influences transcript stability or translation[34].

Pdf regulatory regions affect plasticity

We next asked whether species-specific *cis*-regulatory activity of *Pdf* is sufficient to influence behaviour. We initially used the *D. melanogaster* and *D. sechellia Pdf* 5′-regulatory regions to generate Pdf neuron drivers to induce 'strong' (*D. melanogaster Pdf-Gal4*) or 'weak' (*D. sechellia Pdf-Gal4*) RNA interference (RNAi) of *Pdf*[31], validating the distinct efficacy of knockdown with smFISH (Extended Data Fig. 8). Under both 12:12 and 16:8 h LD, *DmelPdf-Gal4>Pdf^{RNAi}* flies showed a marked advance in evening peak time relative to controls (Fig. 4a–c). Under 12:12 h LD, there was no difference in the degree of evening peak advance between knockdown treatments. By contrast, under 16:8 h LD, *DsecPdf-Gal4>Pdf^{RNAi}* flies showed a smaller, non-significant, decrease in evening peak time relative to control animals, with a notable increase in variance (Fig. 4a–c). Importantly, under 16:8 h LD, the difference between the *Pdf^{RNAi}* genotypes—of otherwise identical genetic background—was significant. These results indicate that the level (and possibly temporal dynamics) of *Pdf* expression is sufficient to affect evening peak plasticity. We also quantified the predawn activity (Fig. 4d) of these flies under 12:12 h LD. Both *DmelPdf-Gal4>Pdf^{RNAi}* and *DsecPdf-Gal4>Pdf^{RNAi}* flies exhibited reduced predawn activity relative to controls. However, *DmelPdf-Gal4>Pdf^{RNAi}* and *DsecPdf-Gal4>Pdf^{RNAi}* flies did not show significant differences in predawn activity following post hoc correction for multiple comparisons.

To test explicitly whether divergence of *Pdf cis*-regulatory regions is sufficient to explain species' behavioural differences, we rescued Pdf expression in a *Pdf*-null *D. melanogaster* background with transgenes containing either the *D. melanogaster* or *D. sechellia Pdf* 5′-regulatory region fused to the *D. melanogaster Pdf* coding sequence. Under 12:12 h LD, rescue strains showed typical patterns of activity, with evening peaks

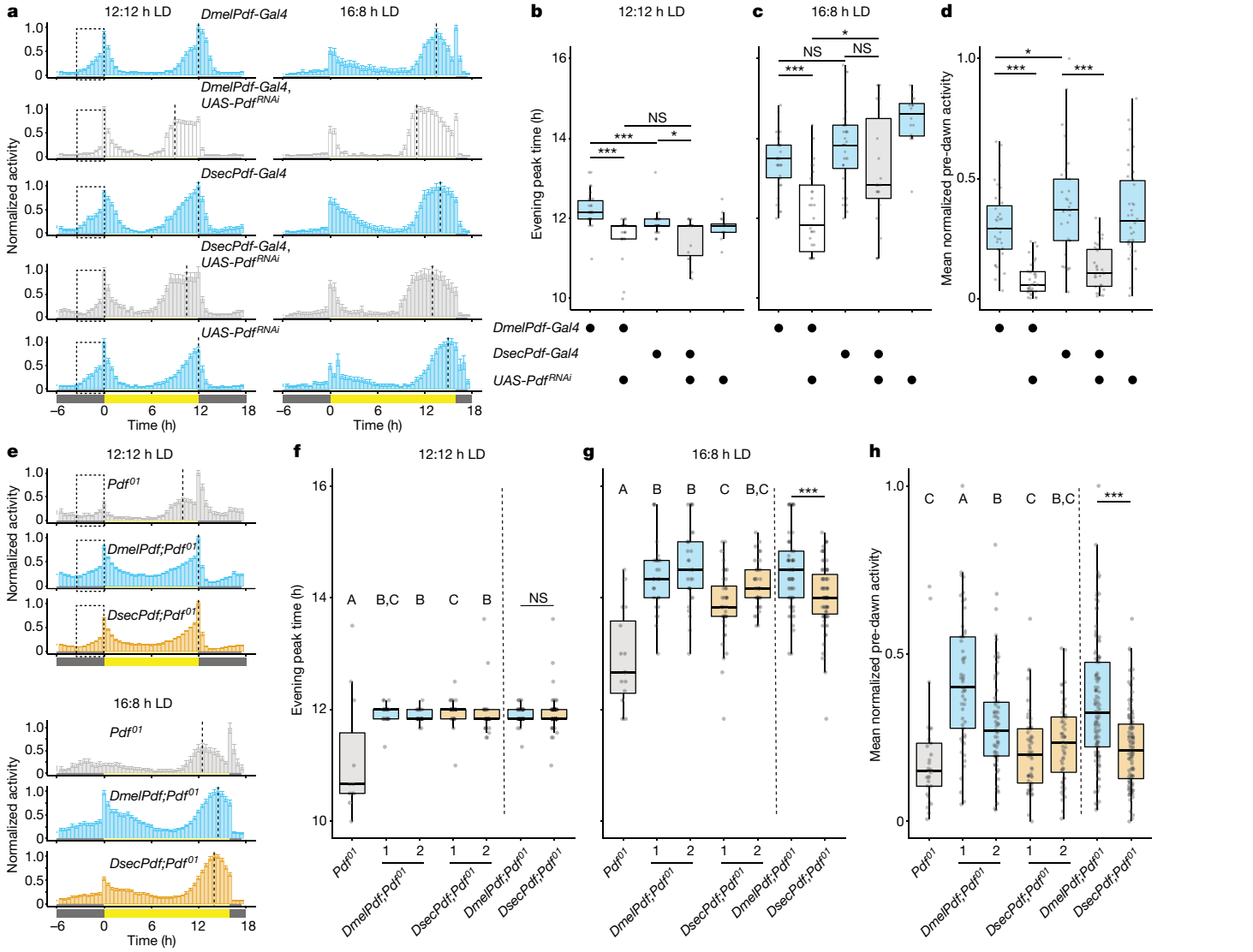

Fig. 4 | Species-specific *Pdf* regulatory regions contribute to divergent evening peak plasticity and morning activity. a, Mean normalized activity of the indicated *Dmel* genotypes under 12:12 h LD (left) and 16:8 h LD (right). *n*: 12:12 h LD, *DmelPdf-Gal4*/+ (31), *DsecPdf-Gal4*/+ (29), *UAS-Pdf*^{RNAi}/+ (47), *DmelPdf-Gal4*/*UAS-Pdf*^{RNAi} (34), *DsecPdf-Gal4*/*UAS-Pdf*^{RNAi} (30); 16:8 h LD, *DmelPdf-Gal4*/+ (34), *DsecPdf-Gal4*/+ (32), *UAS-Pdf*^{RNAi}/+ (16), *DmelPdf-Gal4*/*UAS-Pdf*^{RNAi} (31), *DsecPdf-Gal4*/*UAS-Pdf*^{RNAi} (24). **b**,**c**, Evening peak time for the flies shown in **a** under 12:12 h LD (**b**) and 16:8 h LD (**c**). **d**, Mean normalized predawn activity for the genotypes shown in **a** under 12:12 h LD. **e**, Mean normalized activity of the *Pdf* mutant and *Pdf*-rescue genotypes under 12:12 h LD (top) and 16:8 h LD (bottom) (combined data from two independent lines). *n*: 12:12 h LD, *Pdf*^{01} (30); *DmelPdf,Pdf*^{01} (89); *DsecPdf,Pdf*^{01} (86); 16:8 h LD, *Pdf*^{01} (16), *DmelPdf,Pdf*^{01} (59); *DsecPdf,Pdf*^{01} (79). **f**,**g**, Evening peak time for flies under 12:12 h LD (**f**) and 16:8 h LD (**g**) shown in **e**. *n*: *Pdf*^{01} (16); *DmelPdf,Pdf*^{01} no. 1 (29); *DmelPdf,Pdf*^{01} no. 2 (30); *DsecPdf,Pdf*^{01} no. 1 (38); *DsecPdf,Pdf*^{01} no. 2 (41). **h**, Mean normalized predawn activity for flies depicted in **e** under 12:12 h LD. *n*: *Pdf*^{01} (30); *DmelPdf*^{1},*Pdf*^{01} (40); *DmelPdf*^{1},*Pdf*^{01} (49); *DsecPdf*^{1},*Pdf*^{01} (44); *DsecPdf*^{2},*Pdf*^{01} (42). **b**–**d**,**f**–**h**, *$P < 0.05$, ***$P < 0.001$ (Wilcoxon tests with Bonferroni correction). **f**–**h**, Results for independent species-specific rescue strains and pooled rescue strains are shown in box plots to the left and right of the dashed line, respectively; letters A–C indicate significant differences, $P < 0.05$ (Wilcoxon tests with Bonferroni correction).

centred around lights-off, whereas *Pdf* mutants showed a significantly advanced evening peak time (Fig. 4e,f). Under 16:8 h LD, rescue strains showed greater evening peak plasticity than *Pdf* mutants (Fig. 4g). Importantly, those containing the *D. melanogaster Pdf* 5′-regulatory region showed slightly, but significantly, greater evening peak delay than those with the *D. sechellia* 5′-regulatory sequence (Fig. 4g). We also recorded substantial predawn activity in *D. melanogaster* 5′-regulatory rescue strains compared with *Pdf* mutants under 12:12 h LD (Fig. 4h), but observed a lower increase in those expressing *Pdf* under the *D. sechellia* 5′-regulatory region (Fig. 4h). Importantly, there is again a significant difference between species-specific rescue strains. Together, these results support a contribution of *Pdf cis*-regulatory divergence to species differences in both evening peak plasticity and morning activity.

Pdf regulatory region sequence evolution

To determine whether the *Pdf* 5′-regulatory sequence exhibits evolutionary signatures, we constructed a maximum-likelihood phylogeny of sequences of this region from *D. melanogaster*, *D. sechellia*, *D. simulans* and *D. mauritiana* strains, rooted with sequences from more distant drosophilids (Fig. 5a). Unlike the species tree, *D. sechellia Pdf* 5′-regulatory sequences formed a monophyletic group, whereas the cosmopolitan *D. melanogaster* and *D. simulans* sequences clustered, representing the most derived sequences. *D. mauritiana* and Madagascan *D. simulans* strains showed closer similarity to *D. sechellia* sequences than cosmopolitan *D. melanogaster* and *D. simulans*, potentially reflecting inter- and intraspecific variation between populations

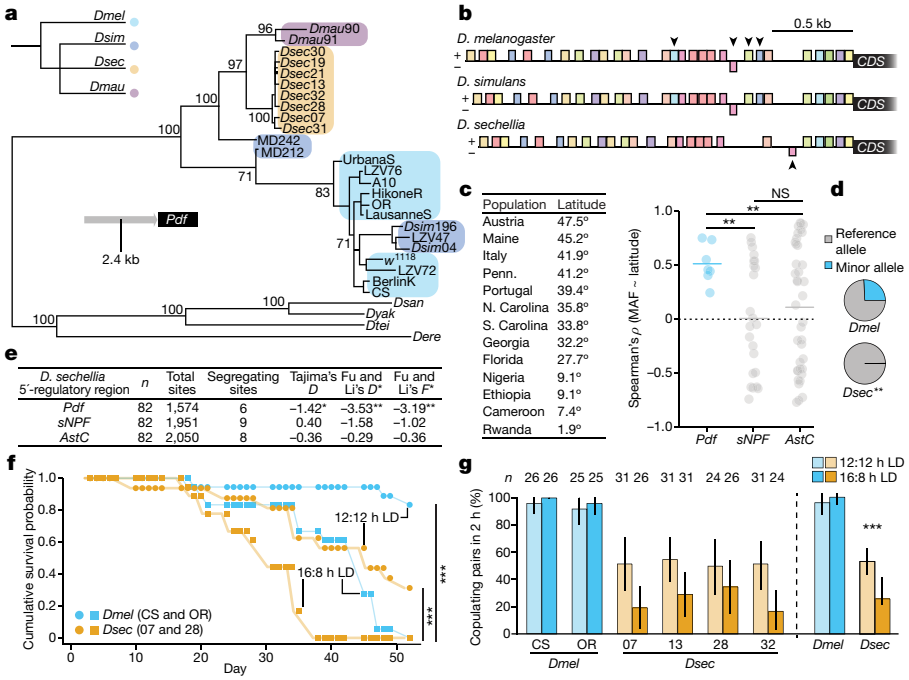

Fig. 5 | Evidence for selection on the *Pdf* 5′-regulatory sequence and fitness effects. a, Maximum-likelihood phylogeny of *Pdf* 5′-regulatory sequences from the *D. melanogaster* subgroup (including *D. mauritiana* and *D. simulans*; species tree top left), rooted with sequences from *Drosophila santomea*, *Drosophila yakuba*, *Drosophila teissieri* and *Drosophila erecta*. Bootstrap support is shown for key internal nodes. **b**, Predicted motifs in the *Pdf* 5′-regulatory sequence, shown as coloured boxes on the +/− strands. *Dmel*/*Dsim*- and *Dsec*-specific motifs are marked with downwards and upwards arrowheads, respectively. **c**, Left, approximate latitude for *Dmel* populations[36]; right, significant differences in the distribution of correlation coefficients for MAF of all variable sites in the putative regulatory sequences of *Pdf* and control genes relative to latitude (*t*-test). **d**, Average MAF of variable sites in the *Pdf* 5′-regulatory sequence (from **c**) in laboratory *Dsec* and *Dmel* strains from **a**. Variable sites are significantly under-represented in *Dsec* relative to *Dmel* (Fisher's exact test). **e**, Sequence-based tests of neutrality in the *Dsec* putative regulatory sequences of *Pdf* and control genes. Tajima's *D*- and Fu and Li's *D**- and *F**-statistics were calculated using 82 *D. sechellia* haplotypes[42]. **f**, Cumulative survival probability for species maintained at the indicated photoperiods. No significant differences were observed between strains of the same species by photoperiod (Fisher's exact test, all $P > 0.05$), and were thus pooled and compared using a log-rank test. **g**, Percentage of copulating pairs for *Dmel* and *Dsec* after 2 h for flies acclimated to 12:12 h LD and 16:8 h LD; 95% confidence intervals were calculated using 1,000 bootstraps. Because there were no differences between strains, we pooled these by species, finding a significant effect in *Dsec* (right, Fisher's exact test). **c**–**g**, $^{*}P < 0.05$, $^{**}P < 0.01$, $^{***}P < 0.001$.

at different latitudes. Motif enrichment analysis[35] identified putative regulatory sequences in these species' 5′ regions. Although all motifs were shared among *D. melanogaster* and *D. simulans* sequences, four were degenerated or absent in *D. sechellia* and one site was unique to this species (Fig. 5b), potentially affecting its activity through the loss (or gain) of transcription factor-binding sites.

We next investigated whether sequence divergence between the *D. melanogaster* and *D. sechellia* 5′-regulatory sequences results from natural selection. We first determined whether variants within the *D. melanogaster Pdf* 5′-regulatory region are associated with higher degrees of evening peak plasticity observed with increasing latitudes[9]. Using single-nucleotide variant frequencies in the genomes of globally distributed *D. melanogaster* populations[36], we chose 13 populations representing a wide range of latitudes (Fig. 5c). We correlated minor allele frequency (MAF) across all variable sites detected within the *Pdf* 5′-regulatory sequence with the estimated latitude of the population collection site. Because correlations could reflect the underlying population structure as a result of *D. melanogaster*'s demographic history during emigration from its native African range[37], as controls we repeated this analysis for a 2.4 kb 5′ region of two other neuropeptide genes, *sNPF* and *AstC*. A positive correlation was consistently observed between population latitude and MAF for each variable site within the *Pdf* 5′-regulatory region, but not for controls (Fig. 5c). These comparisons indicate that the effect of latitude on MAF of *Pdf* 5′-regulatory variants is different from that expected due to demography alone, suggesting a role for selection on these sites in *D. melanogaster*, similar to clinal variation in other circadian genes[38–41]. Among laboratory *D. melanogaster* strains, these single-nucleotide variants occur with an approximate MAF of 25%, but none were present in *D. sechellia* strains (Fig. 5d), consistent with a potential function of these variants in increasing evening peak plasticity.

To test for signs of selection within the *D. sechellia* population, we used 82 *Pdf* 5′-regulatory sequences (plus *sNPF* and *AstC* control sequences) from individuals recently sampled from the Seychelles[42] to calculate Tajima's *D*- and Fu and Li's *D**- and *F**-statistics[40]. All three statistics were significantly negative for *Pdf*, but not for control genes, consistent with recent directional selection acting on this circadian gene (Fig. 5e). Thus, selection might also act to reduce aspects of circadian plasticity at the equator.

Plasticity affects reproductive fitness

To identify a potential mechanism by which natural selection acts, we asked whether plasticity in circadian activity impacts fitness. We first examined lifespan, which is impacted by photoperiod in other animals[43] and probably affects lifetime reproductive output. Both *D. melanogaster* and *D. sechellia* maintained under 16:8 h LD showed a significant reduction in lifespan relative to those under 12:12 h LD (Fig. 5f and Extended Data Fig. 9a,b). However, the detrimental effect of longer photoperiod was not observed until several weeks had elapsed, by which time flies could certainly reproduce, making it less likely to impact fitness in nature.

Circadian rhythms are important for synchronization of sexual behaviour among conspecifics[6,44]. We therefore reasoned that if evening peak plasticity (or the lack thereof) influences copulation success, it might affect fitness. We acclimated male and female virgins to 12:12 and 16:8 h LD for 4 days and observed copulation rates among pairs over a 2 h period after lights-on (Fig. 5g). For *D. melanogaster*, we observed no difference in copulation rates between treatments (Fig. 5g). By contrast, for all *D. sechellia* strains, there was a consistent reduction in copulation rate for flies acclimated to 16:8 h LD (Fig. 5g, left). Pooling of strains by species showed a significant decrease in overall copulation by *D. sechellia* acclimated to 16:8 h LD, but not by *D. melanogaster* (Fig. 5g, right). For some strains, this reduction persisted for several days (Extended Data Fig. 9c). These results demonstrate that *D. sechellia*'s reproductive success—and thus, probably its fitness—is influenced by its lack of evening peak plasticity when exposed to extended photoperiods that it would never experience in nature. By contrast, *D. melanogaster*'s behavioural plasticity could allow it to circumvent these negative effects.

Discussion

Identifying the mechanisms of behavioural plasticity is key to understanding how organisms have evolved to inhabit variable environments and to predict how they will persist in increasingly unstable ones[45]. We have characterized a circadian plasticity difference in drosophilids, providing a rare example of linking changes in gene function, central neuron populations and behavioural divergence.

In *D. melanogaster*, Pdf is required in the l-LNvs for photoperiod plasticity[19], and interspecific spatial differences in Pdf expression exist[28], notably in high-latitude species in which Pdf is restricted to the l-LNvs[10,46]. These observations, combined with our analyses, point to the *Pdf* locus as a hotspot of evolution. Given Pdf's terminal placement as an effector gene of the clock network[21], its role in broad synchronization of circadian clock neurons[47] and its strong influence on circadian behaviours, changes in the *cis*-regulation of *Pdf* expression might represent a minimally pleiotropic means of introducing plasticity into the clock neuronal network.

A single locus clearly does not explain the entirety of species differences in plasticity, as is true of most behaviours[48]. There are almost certainly contributions of additional genes that we have not tested and/or more complex genetic interactions that we cannot identify with our screen design. Beyond the *cis*-regulatory differences in *Pdf* characterized here, the translation[21], transport and secretion of this neuropeptide[49] are all potentially subject to divergent regulation.

D. sechellia also shows greatly reduced morning activity compared with other drosophilids. This phenotype is similar to that observed in *D. melanogaster Pdf* mutants[50], and species-specific *Pdf* rescue in *D. melanogaster* indicates a contribution of *cis*-regulatory divergence of the locus. That our candidate screen did not find an effect of the *Pdf* locus itself in this difference might reflect coevolution of the *Pdf* 5′-regulatory region and its *trans*-acting factors, which could be masked in a hybrid genetic background. Indeed, our screen identified several genes with the ability to regulate *Pdf* expression in *trans*, highlighting a different evolutionary trajectory to evening peak plasticity divergence that nevertheless converges on this neuropeptide. The morning and evening oscillators partially overlap in function, sharing synaptic feedback[19,51], with both being required for long-photoperiod adaptation[27]. Potential mechanistic and evolutionary connections between evening peak plasticity and morning activity require further exploration. Moreover, the evolutionary consequences, if any, of reduced morning peak activity in *D. sechellia* remain unclear. These issues might be illuminated by analyses of the circadian pattern of other behaviours of this species (and its sympatric sister species), such as courtship or feeding, which could constitute further barriers to reproduction[52].

Why has *D. sechellia* lost evening peak plasticity? One hypothesis is that, in a constant photoperiod, selection to maintain plasticity mechanisms is relaxed, leading these to degenerate over time. Alternatively, in stable environments, plasticity might come at a fitness cost, leading selection to favour its loss under constant photoperiods—for example, to enhance the robustness of circadian activity. Regardless, our view of *D. sechellia*'s specialization should expand beyond evolution of host fruit preference to restriction to an equatorial environment. Indeed, *D. sechellia*'s circadian phenotype might contribute to its endemism, despite the wider range of *M. citrifolia*[53]. Exploration of the impact of differences in circadian plasticity mechanisms on latitudinal constraint of other species seems warranted.

Online content

Any methods, additional references, Nature Portfolio reporting summaries, source data, extended data, supplementary information, acknowledgements, peer review information; details of author contributions and competing interests; and statements of data and code availability are available at https://doi.org/10.1038/s41586-024-08056-x.

1. Rieger, D., Stanewsky, R. & Helfrich-Forster, C. Cryptochrome, compound eyes, Hofbauer-Buchner eyelets, and ocelli play different roles in the entrainment and masking pathway of the locomotor activity rhythm in the fruit fly *Drosophila melanogaster*. *J. Biol. Rhythms* **18**, 377–391 (2003).
2. Auer, T. O., Shahandeh, M. P. & Benton, R. *Drosophila sechellia*: a genetic model for behavioral evolution and neuroecology. *Annu. Rev. Genet.* **55**, 527–554 (2021).
3. Roca, I. T. et al. Shifting song frequencies in response to anthropogenic noise: a meta-analysis on birds and anurans. *Behav. Ecol.* **27**, 1269–1274 (2016).
4. Caldwell, A. J., While, G. M. & Wapstra, E. Plasticity of thermoregulatory behaviour in response to the thermal environment by widespread and alpine reptile species. *Anim. Behav.* **132**, 217–227 (2017).
5. Muraro, N. I., Pirez, N. & Ceriani, M. F. The circadian system: plasticity at many levels. *Neuroscience* **247**, 280–293 (2013).
6. Wang, G. et al. Clock genes and environmental cues coordinate *Anopheles* pheromone synthesis, swarming, and mating. *Science* **371**, 411–415 (2021).
7. Horn, M. et al. The circadian clock improves fitness in the fruit fly, *Drosophila melanogaster*. *Front. Physiol.* **10**, 1374 (2019).
8. Hardeland, R. & Stange, G. Comparative studies on the circadian rhythms of locomotor activity of 40 *Drosophila* species. *J. Interdiscipl. Cycle Res.* **4**, 353–359 (1973).
9. Rieger, D., Peschel, N., Dusik, V., Glotz, S. & Helfrich-Forster, C. The ability to entrain to long photoperiods differs between 3 *Drosophila melanogaster* wild-type strains and is modified by twilight simulation. *J. Biol. Rhythms* **27**, 37–47 (2012).
10. Beauchamp, M. et al. Closely related fruit fly species living at different latitudes diverge in their circadian clock anatomy and rhythmic behavior. *J. Biol. Rhythms* **33**, 602–613 (2018).
11. Bywalez, W. et al. The dual-oscillator system of *Drosophila melanogaster* under natural-like temperature cycles. *Chronobiol. Int.* **29**, 395–407 (2012).
12. Matute, D. R., Gavin-Smyth, J. & Liu, G. Variable post-zygotic isolation in *Drosophila melanogaster*/*D. simulans* hybrids. *J. Evol. Biol.* **27**, 1691–1705 (2014).
13. Lachaise, D. et al. in *Historical Biogeography of the Drosophila melanogaster Species Subgroup* (eds. Hecht, M. K., Wallace, B. & Prance, G. T.) 159–225 (Plenum, 1988).
14. Dean, M. D. & Ballard, J. W. Linking phylogenetics with population genetics to reconstruct the geographic origin of a species. *Mol. Phylogenet. Evol.* **32**, 998–1009 (2004).
15. Hardin, P. E. Molecular genetic analysis of circadian timekeeping in *Drosophila*. *Adv. Genet.* **74**, 141–173 (2011).
16. Hermann-Luibl, C. & Helfrich-Forster, C. Clock network in *Drosophila*. *Curr. Opin. Insect Sci.* **7**, 65–70 (2015).
17. Vaze, K. M. & Helfrich-Forster, C. The neuropeptide PDF is crucial for delaying the phase of *Drosophila*'s evening neurons under long Zeitgeber periods. *J. Biol. Rhythms* **36**, 442–460 (2021).
18. Yoshii, T. et al. The neuropeptide pigment-dispersing factor adjusts period and phase of *Drosophila*'s clock. *J. Neurosci.* **29**, 2597–2610 (2009).
19. Schlichting, M. et al. A neural network underlying circadian entrainment and photoperiodic adjustment of sleep and activity in *Drosophila*. *J. Neurosci.* **36**, 9084–9096 (2016).
20. Peschel, N., Chen, K. F., Szabo, G. & Stanewsky, R. Light-dependent interactions between the *Drosophila* circadian clock factors Cryptochrome, Jetlag, and Timeless. *Curr. Biol.* **19**, 241–247 (2009).
21. Gunawardhana, K. L. & Hardin, P. E. VRILLE controls PDF neuropeptide accumulation and arborization rhythms in small ventrolateral neurons to drive rhythmic behavior in *Drosophila*. *Curr. Biol.* **27**, 3442–3453 (2017).
22. Mezan, S., Feuz, J. D., Deplancke, B. & Kadener, S. PDF signaling is an integral part of the *Drosophila* circadian molecular oscillator. *Cell. Rep.* **17**, 708–719 (2016).
23. Grima, B., Chelot, E., Xia, R. & Rouyer, F. Morning and evening peaks of activity rely on different clock neurons of the *Drosophila* brain. *Nature* **431**, 869–873 (2004).
24. Delventhal, R. et al. Dissection of central clock function in *Drosophila* through cell-specific CRISPR-mediated clock gene disruption. *eLife* **8**, e48308 (2019).
25. Stoleru, D., Peng, Y., Agosto, J. & Rosbash, M. Coupled oscillators control morning and evening locomotor behaviour of *Drosophila*. *Nature* **431**, 862–868 (2004).

26. Sheeba, V., Gu, H., Sharma, V. K., O'Dowd, D. K. & Holmes, T. C. Circadian- and light-dependent regulation of resting membrane potential and spontaneous action potential firing of *Drosophila* circadian pacemaker neurons. *J. Neurophysiol.* **99**, 976–988 (2008).
27. Menegazzi, P. et al. A functional clock within the main morning and evening neurons of *D. melanogaster* is not sufficient for wild-type locomotor activity under changing day length. *Front. Physiol.* **11**, 229 (2020).
28. Hermann, C. et al. The circadian clock network in the brain of different *Drosophila* species. *J. Comp. Neurol.* **521**, 367–388 (2013).
29. Park, J. H. et al. Differential regulation of circadian pacemaker output by separate clock genes in *Drosophila*. *Proc. Natl Acad. Sci. USA* **97**, 3608–3613 (2000).
30. Fernandez, M. P., Berni, J. & Ceriani, M. F. Circadian remodeling of neuronal circuits involved in rhythmic behavior. *PLoS Biol.* **6**, e69 (2008).
31. Herrero, A. et al. Coupling neuropeptide levels to structural plasticity in *Drosophila* clock neurons. *Curr. Biol.* **30**, 3154–3166 (2020).
32. Zhang, L. et al. DN1(p) circadian neurons coordinate acute light and PDF inputs to produce robust daily behavior in *Drosophila*. *Curr. Biol.* **20**, 591–599 (2010).
33. Liang, X., Holy, T. E. & Taghert, P. H. A series of suppressive signals within the *Drosophila* circadian neural circuit generates sequential daily outputs. *Neuron* **94**, 1173–1189 (2017).
34. Ryczek, N., Lys, A. & Makalowska, I. The functional meaning of 5'UTR in protein-coding genes. *Int. J. Mol. Sci.* **24**, 2976 (2023).
35. Bailey, T. L. & Elkan, C. Fitting a mixture model by expectation maximization to discover motifs in biopolymers. *Proc. Int. Conf. Intell. Syst. Mol. Biol.* **2**, 28–36 (1994).
36. Bergland, A. O., Tobler, R., Gonzalez, J., Schmidt, P. & Petrov, D. Secondary contact and local adaptation contribute to genome-wide patterns of clinal variation in *Drosophila melanogaster*. *Mol. Ecol.* **25**, 1157–1174 (2016).
37. Arguello, J. R., Laurent, S. & Clark, A. G. Demographic history of the human commensal *Drosophila melanogaster*. *Genome Biol. Evol.* **11**, 844–854 (2019).
38. Khatib, L., Subasi, B. S., Fishman, B., Kapun, M. & Tauber, E. Unveiling subtle geographical clines: phenotypic effects and dynamics of circadian clock gene polymorphisms. *Biology* **12**, 858 (2023).
39. Lamaze, A. et al. A natural timeless polymorphism allowing circadian clock synchronization in "white nights". *Nat. Commun.* **13**, 1724 (2022).
40. Tauber, E. et al. Natural selection favors a newly derived timeless allele in *Drosophila melanogaster*. *Science* **316**, 1895–1898 (2007).
41. Deppisch, P. et al. Adaptation of *Drosophila melanogaster* to long photoperiods of high-latitude summers is facilitated by the ls-timeless allele. *J. Biol. Rhythms* **37**, 185–201 (2022).
42. Schrider, D. R., Ayroles, J., Matute, D. R. & Kern, A. D. Supervised machine learning reveals introgressed loci in the genomes of *Drosophila simulans* and *D. sechellia*. *PLoS Genet.* **14**, e1007341 (2018).
43. Li, J. C. & Xu, F. Influences of light-dark shifting on the immune system, tumor growth and life span of rats, mice and fruit flies as well as on the counteraction of melatonin. *Biol. Signals* **6**, 77–89 (1997).
44. Emerson, K. J., Bradshaw, W. E. & Holzapfel, C. M. Concordance of the circadian clock with the environment is necessary to maximize fitness in natural populations. *Evolution* **62**, 979–983 (2008).
45. Ducatez, S., Sol, D., Sayol, F. & Lefebvre, L. Behavioural plasticity is associated with reduced extinction risk in birds. *Nat. Ecol. Evol.* **4**, 788–793 (2020).
46. Menegazzi, P. et al. Adaptation of circadian neuronal network to photoperiod in high-latitude European drosophilids. *Curr. Biol.* **27**, 833–839 (2017).
47. Shafer, O. T. et al. Widespread receptivity to neuropeptide PDF throughout the neuronal circadian clock network of *Drosophila* revealed by real-time cyclic AMP imaging. *Neuron* **58**, 223–237 (2008).
48. York, R. A. Assessing the genetic landscape of animal behavior. *Genetics* **209**, 223–232 (2018).
49. Ding, K. et al. Imaging neuropeptide release at synapses with a genetically engineered reporter. *eLife* **8**, e46421 (2019).
50. Renn, S. C., Park, J. H., Rosbash, M., Hall, J. C. & Taghert, P. H. A *pdf* neuropeptide gene mutation and ablation of PDF neurons each cause severe abnormalities of behavioral circadian rhythms in *Drosophila*. *Cell* **99**, 791–802 (1999).
51. Duhart, J. M. et al. Circadian structural plasticity drives remodeling of E cell output. *Curr. Biol.* **30**, 5040–5048 (2020).
52. Shahandeh, M. P., Pischedda, A. & Turner, T. L. Male mate choice via cuticular hydrocarbon pheromones drives reproductive isolation between *Drosophila* species. *Evolution* **72**, 123–135 (2018).
53. Razafimandimbison, S. G., McDowell, T. D., Halford, D. A. & Bremer, B. Origin of the pantropical and nutriceutical *Morinda citrifolia* L. (Rubiaceae): comments on its distribution range and circumscription. *J. Biogeogr.* **37**, 520–529 (2010).

Methods

Drosophila strains and rearing

All flies were reared on a wheat flour/yeast/fruit juice medium in non-overlapping 2 week cycles, and kept in 12:12 h LD at 25 °C. For *D. sechellia* strains, we added an additional mixture of instant *Drosophila* medium (Formula 4-24 blue, Carolina bio-supply) mixed with noni juice (Raab Vitalfood).

For comparisons of the circadian behaviour of *D. melanogaster*, *D. sechellia*, *D. simulans* and *D. mauritiana*, at least two wild-type strains of each species were used (*Dmel*CS, *Dmel*OR, *Dmel*LZV L72, *Dmel*LZV L76, *Dsec*07, *Dsec*28, *Dsim*MD221, *Dsim*MD242, *Dmau*90 and *Dmau*91). To screen candidate genes for effects on circadian behaviour differences between *D. melanogaster* and *D. sechellia*, we used *D. melanogaster* strains containing loss-of-function mutations for genes previously associated with circadian behaviour phenotypes. A list of fly strains and their hybridization success (when applicable) is provided in Supplementary Table 1. When strains were not available (*vrille*) or not hybridizable (*Jet* and *timeless*), we used *D. melanogaster* deficiency strains containing engineered chromosomal deletions spanning the region of a candidate gene (in addition to many other loci)[54]. In the case of *timeless*, a deficiency strain did not hybridize either. The *Pdf* strain we used is the Pdf^{01} allele[50] in the Canton-S genetic background (provided by C. Förster, University of Würzburg), because we were unable to hybridize the original Pdf^{01} strain. To confirm that the effect we observed (Extended Data Fig. 3) was not due to a difference in *D. melanogaster* genetic background, we compared hybrids made with this Pdf^{01} strain to the same parental Canton-S (denoted here as *Dmel*CS^{W}, where W represents Würzburg), which showed predawn activity and evening peak plasticity qualitatively similar to our *Dmel*CS strain (Extended Data Fig. 4). To visualize the collection sites of these strains, we generated a world map using the R package 'maps'.

Hybrid crosses and circadian candidate gene screening

We generated *D. melanogaster*/*D. sechellia* hybrids as previously described[55]. In brief, hours-old virgin females were crossed to males that were collected as virgins and aged at high density (15–20 flies) for 5–7 days. To increase interactions between flies, we pushed a plug into the vial to leave a 2–3 cm space above the food surface. These crosses yielded only sterile, but viable, males. This method does not allow us to test sex-linked candidate genes, including the core transcriptional feedback loop member *period*[56] and the Pdf receptor gene, *Pdfr*[47].

Drosophila activity monitoring

For all activity measurements, we used 1–3-day-old males in the *Drosophila* activity monitor system[57] in small incubators that continuously regulate light and temperature conditions (TriTech Research, no. DT2-CIRC-TK). In brief, this system uses an infrared beam that bisects a glass tube (5 mm inner diameter, 65 mm length) in which the fly is housed, to record activity as the number of beam crosses per minute. Flies were transferred into tubes under light CO_2 anaesthesia with a 5% sucrose, 2% agar (w/v) solution at one end and capped with a cotton plug at the other. Each monitor recorded the activity of up to 32 flies simultaneously, and multiple monitors were placed in a single incubator. For each genotype, we tested flies in at least two technical replicates.

All flies were first exposed to 7 days of 12:12 h LD and then shifted to one of four extended photoperiod cycles for an additional 7 days—14:10, 16:8, 18:6 or 20:4 h LD—to allow us to measure 12:12 h LD-associated (that is, predawn activity) and extended photoperiod-associated behaviours (that is, evening peak plasticity) for each animal. For assessment of free-running period, flies were exposed to 7 days of DD following 7 days of 12:12 h LD. For each photoperiod regime, we took the average activity of the final 4 days of each 7 day period. The initial 3 days were considered an acclimation period. All subsequent analyses were performed in R using the Rethomics package[58]. For activity plots, maximum normalization was performed to standardize all plots to a range of 0–1.

To quantify predawn activity, average normalized activity was calculated for each fly in 30 min bins in the 3 h preceding dawn. To quantify morning and evening peak times, peak activity was identified from the average activity of each fly in 10 min bins during the last 4 days of both the 12:12 h LD and extended photoperiod using custom R scripts (available at github.com/mshahandeh/circ_plasticity). First, a rolling triangular mean was applied to smooth the data, which were then split into two 12 h sections, the first spanning the time around lights-on and the second spanning the time around lights-off (at least 3 h preceding and 3 h after for both). The global peak was identified within each dataset and recorded as the timing of the morning and evening peak, respectively.

For activity plots shown in the figures, average activity is plotted in 30 min bins, with yellow and grey bars at the bottom indicating timing of lights-on and -off, respectively. Error bars indicate the standard error of the mean. For evening peak time, vertical dashed lines indicate the average timing of the evening peak; for predawn activity, dashed boxes highlight the predawn period (3 h before lights-on). For quantifications of both evening peak time and predawn activity, standard box plots were used in which the bold middle line represents the median of the data, the box the interquartile range and the whiskers the remaining quartiles. Outliers are depicted with data points.

smFISH

We used the *Pdf* probe library described previously[59] bound to the Cy5 fluorophore (LubioScience), essentially following a published protocol[60]. Brains were imaged using an inverted confocal microscope (Zeiss LSM 710 or 880) equipped with a ×40 or ×63 oil-immersion objective, and using fixed settings to maximize the comparability of images within experiments. Images were captured using Microsoft ZEN 2.3 SP1 software. Images were processed in Fiji and RNA spots were counted using the Fiji macro RS-FISH[61]. No signal was detected outside of the LNv cell bodies. RNA spot counts between strains within photoperiod treatments were compared using a Wilcoxon rank-sum test followed by post hoc correction for multiple tests[62]. We did not compare between experiments because these flies were dissected, stained and imaged separately. smFISH was repeated for two time points during the morning and evening peaks under both 12:12 and 16:8 h LD to ensure replicability of the overall pattern of expression. We did not pool these data because they are from a separate staining/imaging.

Immunofluorescence

For immunofluorescence of whole-mount *Drosophila* brains, 1–2-day-old males were collected and acclimated to a specific photoperiod for four additional days. To standardize sampling times, we fixed these flies in 4% paraformaldehyde for 2 h at room temperature with gentle agitation before dissection. Brains were dissected and stained essentially as described[63]. Primary and secondary antibodies and concentrations used are provided in Supplementary Table 2. Brains were imaged using an inverted confocal microscope (Zeiss LSM 710 or 880) equipped with a ×20 or ×40 objective, and using fixed settings to maximize the comparability of images. Images were captured using Microsoft ZEN 2.3 SP1 software. To quantify fluorescence, images were processed in Fiji by first creating a maximum-intensity projection *z*-stack, which was thresholded to remove background signal[64]. Relative fluorescence was measured for each set of neurons by structure (that is, LNv soma or s-LNv dorsal axonal projections) as integrated density of pixel intensity, and the average of both hemispheres was recorded for each brain. We compared Pdf immunofluorescence between strains within photoperiod treatments using a Wilcoxon rank-sum test followed by post hoc correction for multiple tests[62]. We did not compare between experiments because these flies were dissected, stained and imaged separately. We repeated immunostainings for two time points

during the morning and evening peaks under both 12:12 and 16:8 h LD, to ensure replicability of the overall pattern of expression. These data cannot be pooled, however, because they are from a separate staining/imaging and produce different fluorescence measurements (arbitrary units).

For comparison of the structural plasticity of s-LNv axonal projections between *D. melanogaster* and *D. sechellia*, we imaged the most dorsal projections during two time points in the light and dark phases (2 and 14 h, respectively) at ×40 with a ×2 digital zoom. We performed Scholl analysis on these images, counting the number of axonal crossings with concentric 10 µm arcs using the Neuroanatomy Fiji plugin[65]. The number of axonal crossings was averaged per hemisphere for each brain and compared using a Wilcoxon rank-sum test. We performed this experiment in two replicates and pooled replicates for analysis because fluorescence intensity was not measured.

Construction of transgenic lines

Approximately 2.4 kb upstream of the *Pdf* start codon was PCR amplified from *D. melanogaster* (*Dmel*CS) or *D. sechellia* (*Dsec*28) gDNA and Gateway cloned into the pDONR221 vector, sequenced verified and subcloned into pHemmarG (Addgene, no. 31221) for CD4:tdGFP reporters, pBPGUw (Addgene, no. 17575) for Gal4 drivers or fused to the *D. melanogaster* (*Dmel*CS) *Pdf* coding sequence in pattB[66] with Gibson assembly, for species-specific rescue constructs. Constructs were injected and integrated into the attP2 landing site (chromosome 3)[67] in the *D. melanogaster* genome by BestGene Inc. Rescue constructs were recombined into the Pdf^{01} background and genotyped with PCR and Sanger sequencing. For elimination of genetic background effects, for each species-specific rescue construct we collected data for two independent insertions. Oligonucleotides used for cloning and sequence verification are listed in Supplementary Table 3.

Pdf gene region sequence comparisons

We PCR amplified and Sanger sequenced the *Pdf* gene region using the oligonucleotides listed in Supplementary Table 3. Sequences were assembled and aligned in SnapGene (www.snapgene.com) using MUSCLE v.3.8.1551 (ref. 68) and visually inspected for alignment errors. *Pdf* coding sequences were translated to an amino acid alignment and visualized using Jalview[69] (v.2.11.2). For 5'-regulatory sequences, we used the R package phangorn to generate maximum-likelihood trees[70], with the modelTest function to identify the best-fitting substitution model and performing standard bootstrapping to obtain support values. The MEME program was used to discover putative regulatory motifs common across *Pdf* 5′-regulatory sequences with $n > 5$ sequences per species[35]. We restricted this analysis to the top ten most significant motifs identified.

Population genetic analysis of *Pdf* 5′-regulatory sequences

For detection of genomic patterns of clinal adaptation in *Pdf* 5′ sequences, we used a dataset of single-nucleotide variants in globally distributed *D. melanogaster* populations[36]. We selected populations from this dataset with a read depth greater than five to ensure confidence in variant frequencies. For each population, we calculated MAF across all variable sites in this region, and for the same-sized region upstream of the start codon of two control neuropeptide genes. Spearman's rho was used to correlate MAF with the latitude of the capital city in each country in which the populations were sampled (precise latitudes were not available). Correlation coefficients for all variable sites within each locus were compared using a *t*-test.

We obtained 41 *D. sechellia* genomes sampled in the Seychelles archipelago from the Sequence Read Archive[42], aligned them to the *D. sechellia* reference genome (ASM438219v2), phasing the data by chromosome (Samtools v.1.19.2), and created consensus sequences for the 82 *Pdf* 5′-regulatory haplotypes. The software DNA sequence polymorphism (v.6) was used to calculate neutrality test statistics, with significance determined by 1,000 coalescence simulations.

Longevity assay

To test for photoperiod-dependent differences in lifespan, we acclimated 1-day-old *Dmel*CS, *Dmel*OR, *Dsec*07 and *Dsec*28 males to either 12:12 h LD or 16:8 h LD. We kept ten flies of each genotype individually in vials containing wheat flour/yeast/fruit juice medium, to which we added an additional mixture of instant *Drosophila* medium (Formula 4-24 blue, Carolina bio-supply), mixed with noni juice for *D. sechellia* or apple cider vinegar (Denner) for *D. melanogaster*. Flies were transferred to fresh vials every 3 days to prevent media from drying out. We recorded for each weekday the number of vials in which a fly died until all flies among one treatment per strain were dead. No significant differences were detected between strains within species (Fisher's exact test, all $P > 0.05$), which were therefore pooled to represent the species for Fig. 5f. We compared cumulative survival probability using the R package 'survival' (ref. 71). We performed a second replicate of these experiments to verify the observed effects (Extended Data Fig. 9).

Copulation assays

To test for photoperiod-dependent differences in copulation rate, we first acclimated 1-day-old virgin *Dmel*CS, *Dmel*OR, *Dsec*07 and *Dsec*28 males and females to either 12:12 or 16:8 h LD for 4 days. We aspirated single females into 25-mm-diameter food vials containing wheat flour/yeast/fruit juice medium, returned them to their respective photoperiods and allowed them to recover for 24 h. The following day, 30 min after lights-on, we aspirated a single male of the same genotype into each tube and pushed the plug into the vial so that pairs had a 2 cm space above the food surface, forcing them to interact. We observed courtship for 2 h, recording successfully and unsuccessfully copulating pairs. We reasoned that a consistent reduction in copulation success over 2 h would be sufficient to affect fitness in the field, in which individual flies interact for only much shorter periods of time[72,73]. We observed no differences between strains within species (Fig. 5g; Fisher's exact test, all $P = 1$), so these data were pooled to represent the species for analysis (Fig. 5g).

To determine whether these differences persisted over the long term, following acclimation to either 12:12 h LD or 16:8 h LD for 4 days, single male–virgin female pairs were aspirated into the same food vials and stored at 25 °C for 3 days, after which the males were removed. Vials that produced offspring were counted as successful copulation. Copulation frequencies within species between treatments were compared using Fisher's exact test.

Data reporting

No statistical methods were used to predetermine sample size. For behavioural experiments, we aimed for a sample size of 25–30 individuals because significant differences are easily detected at these sizes. In the case of our hybrid screen, in which hybrid flies were difficult to produce, we reduced this to 15 individuals per strain but, due to the strong reproductive isolation between species, some genotypes were difficult to cross with *D. sechellia*, resulting in a lower sample size. For image analyses, we obtained images from five brains from each strain per treatment, because this allowed for parallel processing of multiple genotypes and time points. For both behavioural assays and image analyses, data were collected and analysed blind to treatment (species, genotype, sampling time and so on). We did not randomize within experiments, but instead ran all genotypes in parallel for all experiments, with the exception of the hybrid screen, in which the behaviour of hybrids was measured as offspring were successfully obtained from crosses. In this case, test hybrid behaviour was measured at least once in parallel to control hybrids and parental strains. For all experiments, flies were 3–5 days old at the start of the experiment.

Reporting summary

Further information on research design is available in the Nature Portfolio Reporting Summary linked to this article.

Data availability

Data supporting the findings of this study are available at Dryad (https://doi.org/10.5061/dryad.vq83bk42z)[74]. We additionally used *D. melanogaster* single-nucleotide variation data from ref. 36 (data available at https://doi.org/10.5061/dryad.7440s)[75]. We used sequences of *D. sechellia* from ref. 42, available from SRA: SRP113415. To align these sequences, we used the *D. sechellia* reference genome (ASM438219v2). Source Data are provided with this paper.

Code availability

Code used for analyses is available from GitHub (github.com/mshahandeh/circ_plasticity).

54. Cook, R. K. et al. The generation of chromosomal deletions to provide extensive coverage and subdivision of the *Drosophila melanogaster* genome. *Genome Biol.* **13**, R21 (2012).
55. Shahandeh, M. P. & Turner, T. L. The complex genetic architecture of male mate choice evolution between *Drosophila* species. *Heredity (Edinb.)* **124**, 737–750 (2020).
56. Zhou, J., Yu, W. & Hardin, P. E. CLOCKWORK ORANGE enhances PERIOD mediated rhythms in transcriptional repression by antagonizing E-box binding by CLOCK-CYCLE. *PLoS Genet.* **12**, e1006430 (2016).
57. Chiu, J. C., Low, K. H., Pike, D. H., Yildirim, E. & Edery, I. Assaying locomotor activity to study circadian rhythms and sleep parameters in *Drosophila*. *J. Vis. Exp.* **43**, 2157 (2010).
58. Geissmann, Q., Garcia Rodriguez, L., Beckwith, E. J. & Gilestro, G. F. Rethomics: an R framework to analyse high-throughput behavioural data. *PLoS ONE* **14**, e0209331 (2019).
59. Long, X., Colonell, J., Wong, A. M., Singer, R. H. & Lionnet, T. Quantitative mRNA imaging throughout the entire *Drosophila* brain. *Nat. Methods* **14**, 703–706 (2017).
60. Yuan, Y., Padilla, M. A., Clark, D. & Yadlapalli, S. Streamlined single-molecule RNA-FISH of core clock mRNAs in clock neurons in whole mount *Drosophila* brains. *Front. Physiol.* **13**, 1051544 (2022).
61. Bahry, E. et al. RS-FISH: precise, interactive, fast, and scalable FISH spot detection. *Nat. Methods* **19**, 1563–1567 (2022).
62. Holm, S. A simple sequentially rejective multiple test procedure. *Scand. J. Stat.* **6**, 65–70 (1979).
63. Ostrovsky, A., Cachero, S. & Jefferis, G. Clonal analysis of olfaction in *Drosophila*: immunochemistry and imaging of fly brains. *Cold Spring Harb. Protoc.* **2013**, 342–346 (2013).
64. Schindelin, J. et al. Fiji: an open-source platform for biological-image analysis. *Nat. Methods* **9**, 676–682 (2012).
65. Ferreira, T. A. et al. Neuronal morphometry directly from bitmap images. *Nat. Methods* **11**, 982–984 (2014).
66. Bischof, J., Maeda, R. K., Hediger, M., Karch, F. & Basler, K. An optimized transgenesis system for *Drosophila* using germ-line-specific phiC31 integrases. *Proc. Natl Acad. Sci. USA* **104**, 3312–3317 (2007).
67. Markstein, M., Pitsouli, C., Villalta, C., Celniker, S. E. & Perrimon, N. Exploiting position effects and the gypsy retrovirus insulator to engineer precisely expressed transgenes. *Nat. Genet.* **40**, 476–483 (2008).
68. Edgar, R. C. MUSCLE: multiple sequence alignment with high accuracy and high throughput. *Nucleic Acids Res.* **32**, 1792–1797 (2004).
69. Procter, J. B. et al. Alignment of biological sequences with Jalview. *Methods Mol. Biol.* **2231**, 203–224 (2021).
70. Schliep, K. P. phangorn: Phylogenetic analysis in R. *Bioinformatics* **27**, 592–593 (2011).
71. Therneau, T. M. & Grambsch, P. M. *Modelling Survival Data: Extending the Cox Model* (Springer, 2000).
72. Jezovit, J. A., Alwash, N. & Levine, J. D. Using flies to understand social networks. *Front. Neural Circuits* **15**, 755093 (2021).
73. Dukas, R. Natural history of social and sexual behavior in fruit flies. *Sci. Rep.* **10**, 21932 (2020).
74. Shahandeh, M. Data from: circadian plasticity evolves through regulatory changes in a neuropeptide gene. *Dryad* https://doi.org/10.5061/dryad.vq83bk42z (2024).
75. Bergland, A. O. et al. Data from: secondary contact and local adaptation contribute to genome-wide patterns of clinal variation in *Drosophila melanogaster*. *Dryad* https://doi.org/10.5061/dryad.7440s (2015).

Acknowledgements We thank E. Bertolini, C. Förster, D. Matute, J. Saltz, the Bloomington *Drosophila* Stock Center (NIH P40OD018537) and the Developmental Studies Hybridoma Bank (NICHD of the NIH, University of Iowa) for reagents. We thank R. Arguello, E. Bertolini, D. Gatfield and members of the Benton laboratory for discussions and comments on the manuscript. Research in E.N.'s laboratory is supported by the SNSF (no. 310030_189169), and R.B.'s laboratory is supported by the University of Lausanne, an ERC Advanced Grant (no. 833548) and the SNSF (no. 310030B_185377).

Author contributions M.P.S. and R.B. conceived the project. M.P.S. designed, performed and analysed most experiments. L.A. performed hybrid screening and sequencing of the *Pdf* gene region. L.L.D.D. contributed to the experiments shown in Fig. 1c. J.C. contributed to the experiments shown in Extended Data Figs. 3 and 5. R.K. assisted with preliminary behavioural experiments and, together with E.N. and R.B., provided input on experimental design, analysis and interpretation. M.P.S. and R.B. wrote the paper with feedback from all authors.

Competing interests The authors declare no competing interests.

Additional information

Supplementary information The online version contains supplementary material available at https://doi.org/10.1038/s41586-024-08056-x.

Correspondence and requests for materials should be addressed to Michael P. Shahandeh or Richard Benton.

Peer review information *Nature* thanks Charlotte Förster and the other, anonymous, reviewer(s) for their contribution to the peer review of this work. Peer reviewer reports are available.

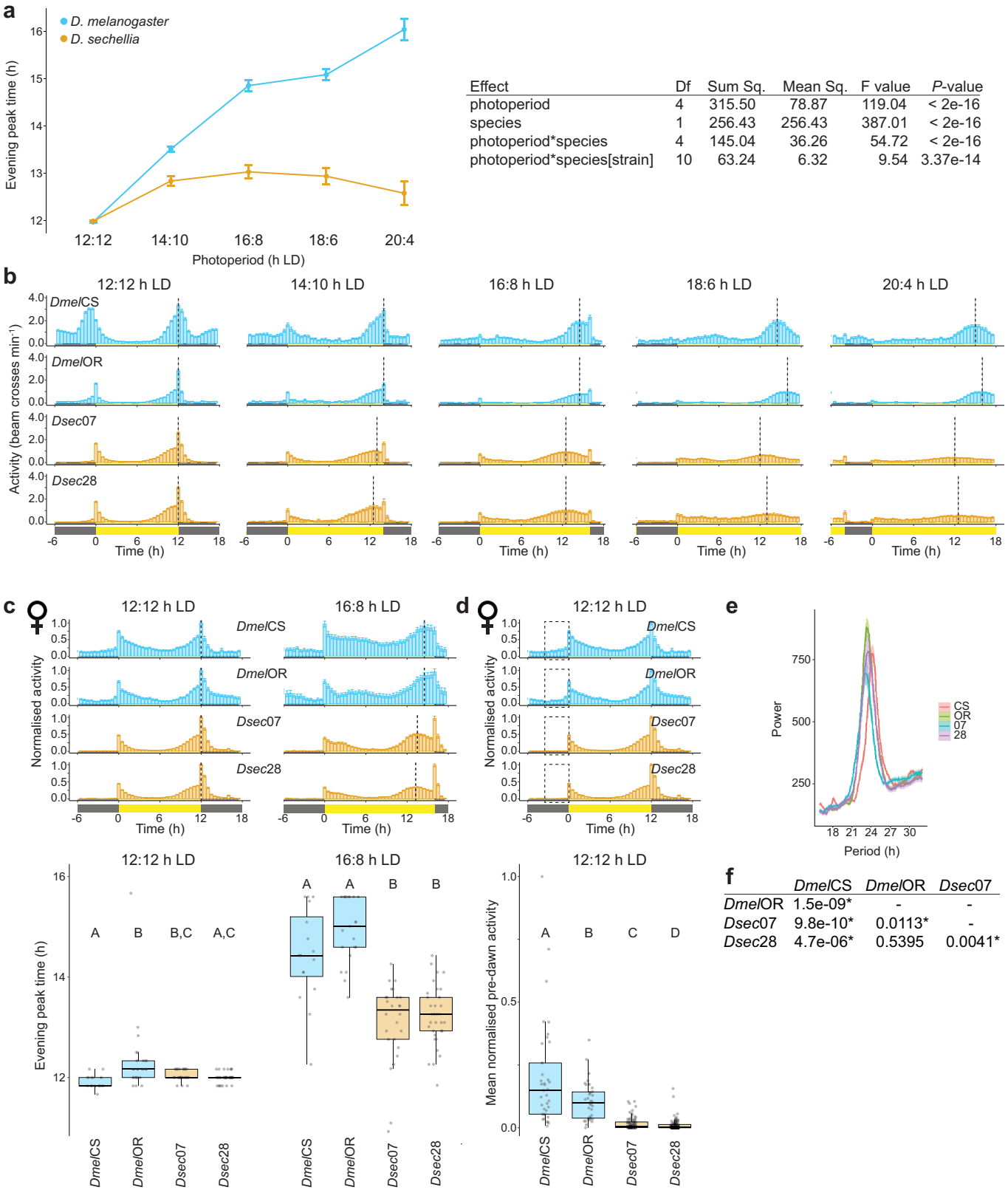

Effect	Df	Sum Sq.	Mean Sq.	F value	*P*-value
photoperiod	4	315.50	78.87	119.04	< 2e-16
species	1	256.43	256.43	387.01	< 2e-16
photoperiod*species	4	145.04	36.26	54.72	< 2e-16
photoperiod*species[strain]	10	63.24	6.32	9.54	3.37e-14

f

	*Dmel*CS	*Dmel*OR	*Dsec*07
*Dmel*OR	1.5e-09*	-	-
*Dsec*07	9.8e-10*	0.0113*	-
*Dsec*28	4.7e-06*	0.5395	0.0041*

Extended Data Fig. 1 | See next page for caption.

Extended Data Fig. 1 | Activity of *D. melanogaster* and *D. sechellia* males and females under different photoperiods. a, Left: reaction norm depicting the interaction between species and photoperiod in determining evening peak time. Points represent species means and error bars represent SEM. Right: results of a two-way nested ANOVA detecting a significant interaction between species and photoperiod in determining evening peak time. **b**, Mean non-normalised activity of flies from Fig. 1c. Vertical dashed lines indicate the average timing of the evening peak for each strain. Error bars represent SEM. Sample sizes as in Fig. 1c. **c**, Top: mean normalised activity of two *D. melanogaster* (CS and OR, blue) and two *D. sechellia* (07 and 28, orange) strains, using female flies, under the indicated photoperiods. Plots depict normalised average activity of the last 4 days of a 7-day photoperiod; for 16:8 h LD, this was preceded by 7 days of 12:12 h LD. Bottom: box plots depict evening peak time quantifications for individual flies under each photoperiod. Here and elsewhere, box plots show the median (bold line), interquartile range (box) and final quartiles (whiskers). Individual data points are overlaid on the box plots; outliers are points that fall beyond the box plot whiskers. Sample sizes (numbers of individual flies) are: 12:12 h LD: CS (37), OR (34), 07 (95), 28 (146); 16:8 h LD: CS (16), OR (21), 07 (30), 28 (33). For **b**-**c**, Vertical dashed lines indicate the average timing of the evening peak for each strain. Here and elsewhere, yellow and grey bars indicate timing of lights-on and lights-off, respectively. Error bars represent SEM. **d**, Mean normalised activity of *D. melanogaster* and *D. sechellia* strains under 12:12 h LD during the morning activity peak (same data from **c**). Top: plots depict average activity of the last 4 days of a 7-day recording period. Dashed boxes highlight the pre-dawn period, 3 h before lights-on. Error bars represent SEM. Bottom: mean normalised activity of individual flies within this pre-dawn period. Sample sizes as in **c**. For **c**-**d**, letters indicate significant differences: $P < 0.05$ (pairwise Wilcoxon test with Bonferroni correction). **e**, Periodogram analysis from 5 days of constant darkness (DD) for *D. melanogaster* (CS and OR) and *D. sechellia* (07 and 28) strains. Period estimates: CS (24.36 h), OR (23.45 h), 07 (23.16 h), 28 (23.57 h). Sample sizes as in Fig. 1e. **f**, Table of *P*-values from all pairwise comparisons of the data in **e** between strains (Wilcoxon test with Bonferroni correction). No species-specific differences were observed.

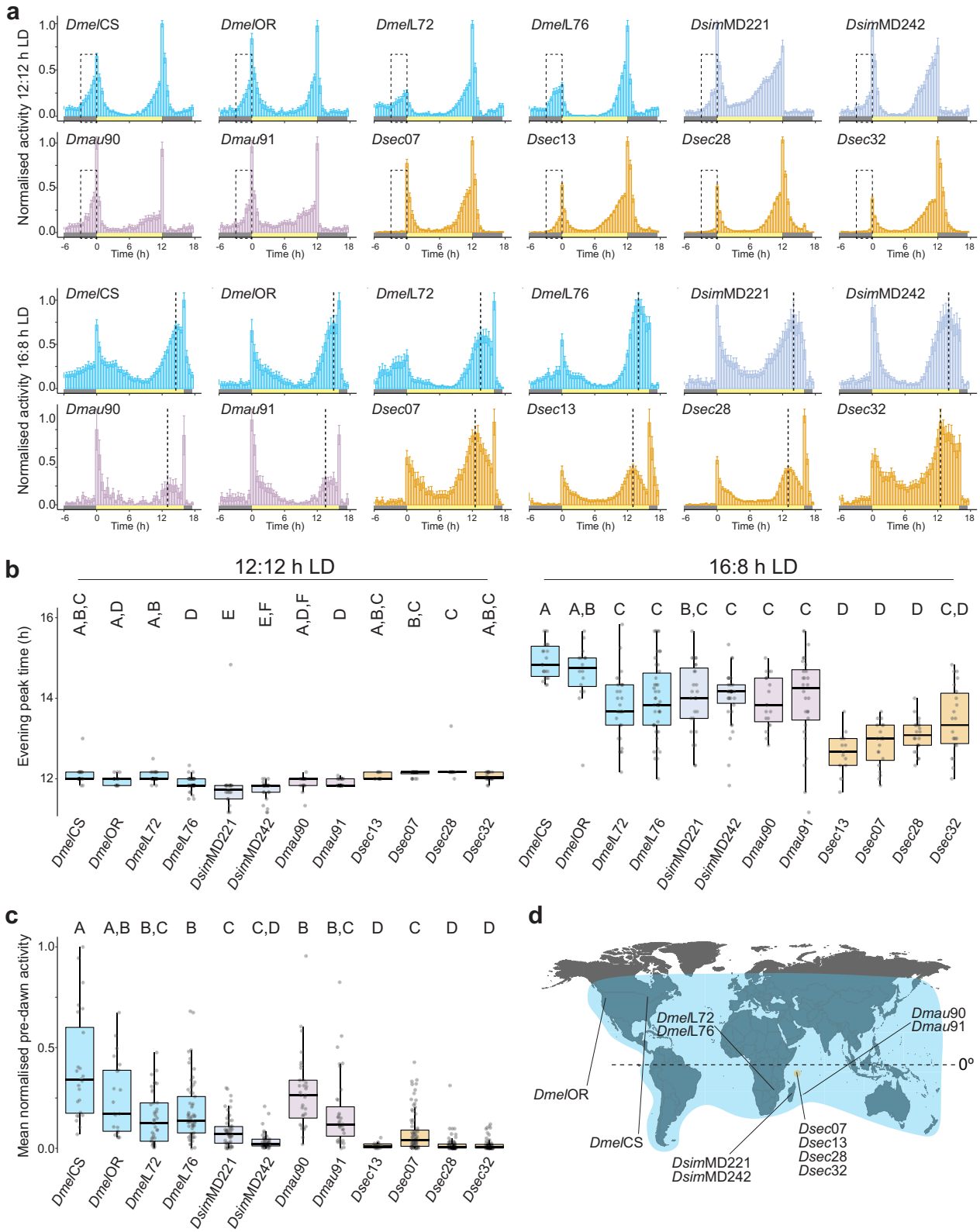

Extended Data Fig. 2 | See next page for caption.

Extended Data Fig. 2 | Tropical *D. melanogaster*, *D. simulans* and *D. mauritiana* strains display prominent evening peak plasticity and morning peak activity. a, Mean normalised activity of laboratory *D. melanogaster* (*Dmel*CS and *Dmel*OR), two recently-collected strains of *D. melanogaster* (*Dmel*L72 and *Dmel*L76, from the Lower Zambezi Valley), *D. simulans* (MD221 and MD242, from Madagascar), *D. mauritiana* (*Dmau*90 and *Dmau*91, from Mauritius) and laboratory *D. sechellia* (*Dsec*07, *Dsec*13, *Dsec*28 and *Dsec*32) under 12:12 h LD (top) and 16:8 h LD (bottom). Plots depict average activity of the last 4 days of a 7-day recording period; for 16:8 h LD, this was preceded by 7 days of 12:12 h LD. Dashed boxes highlight the pre-dawn period, 3 h before lights-on. Dashed lines highlight the average evening peak time. Error bars represent SEM. **b**, Evening peak time for these flies under 12:12 h LD (left) and 16:8 h LD (right). Sample sizes: *Dmel*CS (22), *Dmel*OR (16), *Dmel*L72 (29), *Dmel*L74 (46), *Dsim*MD221 (27), *Dsim*MD242 (34), *Dmau*90 (19), *Dmau*91 (28), *Dsec*07 (19), *Dsec*13 (20), *Dsec*28 (24), *Dsec*32 (22). **c**, Mean normalised activity of individual flies within this pre-dawn period. Sample sizes: *Dmel*CS (24), *Dmel*OR (21), *Dmel*L72 (41), *Dmel*L74 (61), *Dsim*MD221 (57), *Dsim*MD242 (52), *Dmau*90 (33), *Dmau*91 (34), *Dsec*07 (19), *Dsec*13 (82), *Dsec*28 (77), *Dsec*32 (73). **d**, The approximate collection sites of the *D. melanogaster*, *D. simulans*, *D. mauritiana* and *D. sechellia* strains used in **a**-**c**. For **b**-**c**, letters depict significant differences detected between strains (Wilcoxon tests for all pairwise comparisons with Bonferroni correction, $P < 0.05$).

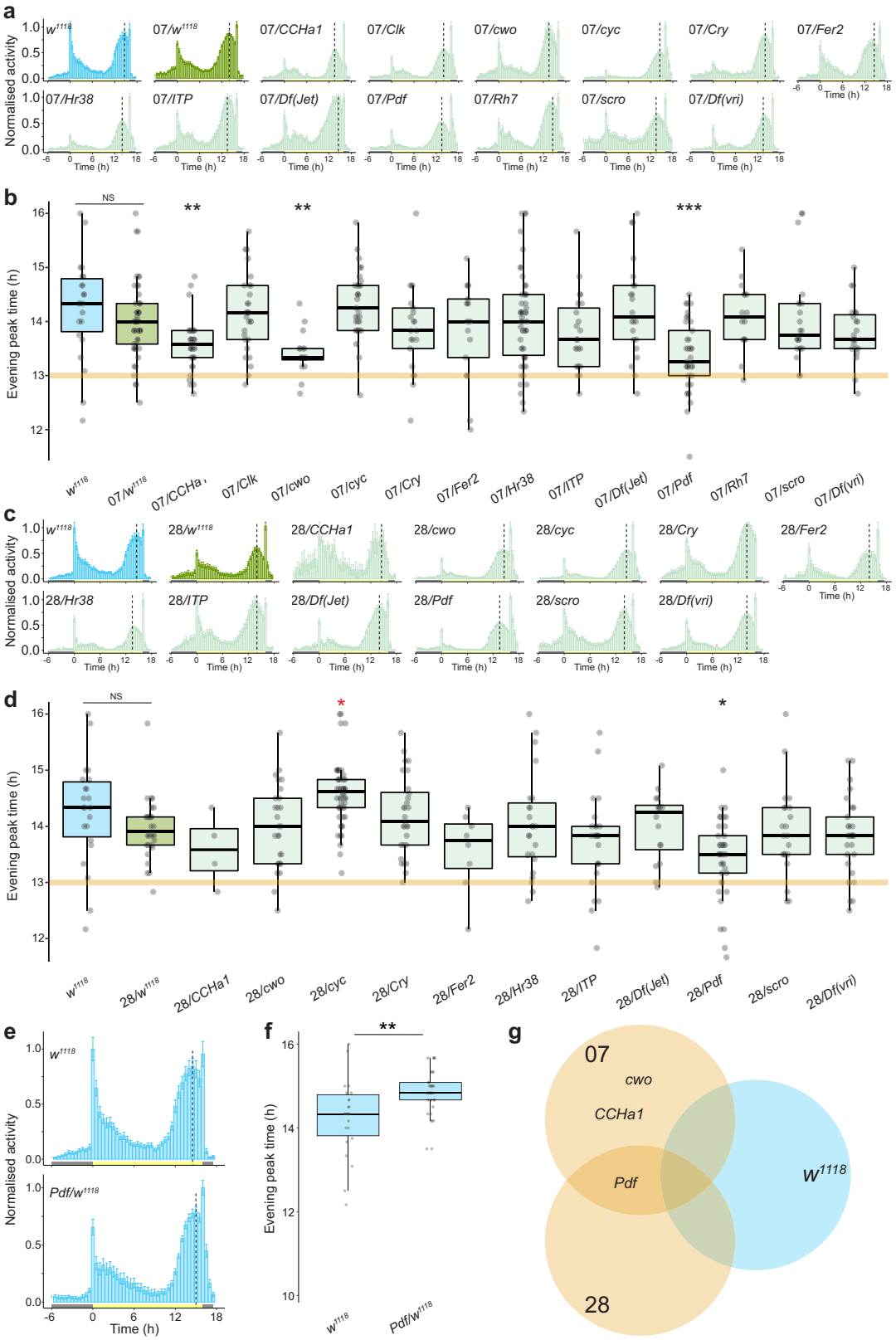

Extended Data Fig. 3 | See next page for caption.

Extended Data Fig. 3 | Screen results for the genetic basis of interspecific differences in evening peak plasticity. a, Mean normalised activity of the indicated control and hybrid genotypes under 16:8 h LD. Plots depict average activity of the last 4 days of a 7-day extended photoperiod, following 7 days of 12:12 h LD. Vertical dashed lines indicate the average timing of the evening peak for each genotype. Error bars represent SEM. Sample sizes: w^{1118} (22), 07/w^{1118} (53), 07/*CCHa1* (34), 07/*Clk* (29), 07/*cwo* (16), 07/*cyc* (33), 07/*Cry* (21), 07/*Fer2* (17), 07/*Hr38* (50), 07/*ITP* (23), 07/*Jet* (22), 07/*Pdf* (37), 07/*Rh7* (16), 07/*scro* (22), 07/*vri* (23), 07 (24). **b**, Evening peak time for the genotypes in **a**. Asterisks indicate significant differences: ** $P < 0.01$ and *** $= P < 0.001$ (Wilcoxon tests comparing each test hybrid to the control hybrid strain (07/w^{1118}) with Bonferroni correction). NS = not significantly different. The orange line marks the median evening peak delay of the *D. sechellia* parental strain (07). **c**, Mean normalised activity of the indicated control and hybrid genotypes under 16:8 h LD. Plots depict average activity of the last 4 days of a 7-day extended photoperiod, following 7 days of 12:12 h LD. Vertical dashed lines indicate the average time of the evening peak for each strain. Error bars represent SEM. Sample sizes: w^{1118} (22), 28/w^{1118} (31), 28/*CCHa1* (4), 28/*cwo* (27), 28/*cyc* (52), 28/*Cry* (28), 28/*Fer* (8), 28/*Hr38* (23), 28/*Itp* (25), 28/*Jet* (16), 28/*Pdf* (40), 28/*scro* (31), 28/*vri* (29), 28 (19). **d**, Evening peak time for the genotypes in **c**. Asterisks indicate significant differences: * $= P < 0.05$ (Wilcoxon tests comparing each test hybrid to the control hybrid strain (28/w^{1118}) with Bonferroni correction). Red asterisk denotes a significant increase in evening peak plasticity. NS = not significantly different. The orange line marks the median evening peak delay of the *D. sechellia* parental strain (28). **e**, Mean normalised activity of hemizygous *D. melanogaster Pdf* mutants (the only mutant that displayed an effect in both hybrid backgrounds) under a 16:8 h LD cycle. Plots depict average activity of the last 4 days of a 7-day extended photoperiod, following 7 days of 12:12 h LD. Vertical dashed lines indicate the average time of the evening peak for each strain. Error bars represent SEM. Sample sizes: w^{1118} (22), *Pdf*/w^{1118} (37). **f**, Evening peak time for the flies depicted in **e**. Pdf^{01} hemizygotes displayed a significant increase in morning peak activity compared to the control strain (w^{1118}). ** $= P < 0.01$ (Wilcoxon test). **g**, Summary of the overlapping hits. A priori, we considered the strongest candidates would display a reduction in evening peak plasticity in both *Dsec*07 and *Dsec*28 hybrids, but not in w^{1118} hemizygotes; only *Pdf* fulfilled these criteria.

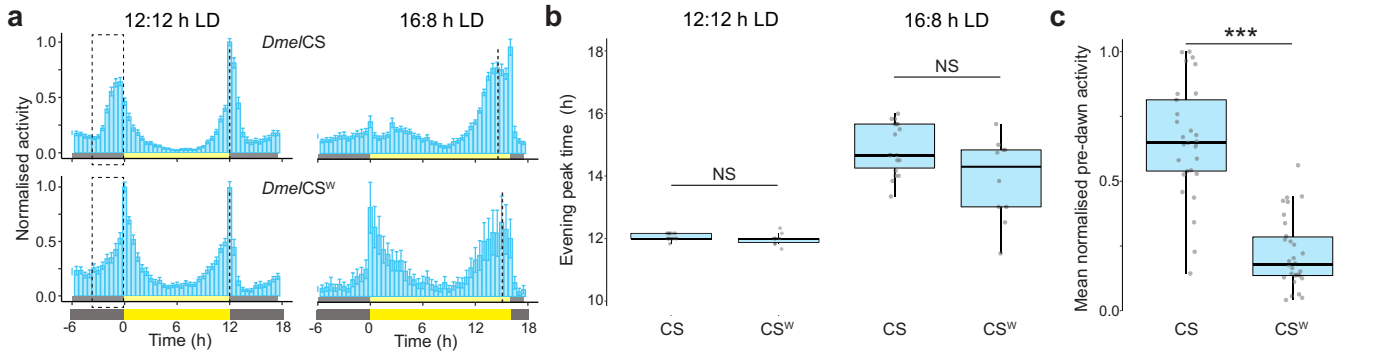

Extended Data Fig. 4 | Qualitatively similar evening peak plasticity and morning peak activity in two Canton-S strains. a, Mean normalised activity of two Canton-S (CS and CS^{W}) strains under 12:12 h (left) and 16:8 h LD (right). Plots depict average activity of the last 4 days of a 7-day extended photoperiod, following 7 days of 12:12 h LD. Vertical dashed lines indicate the average timing of the evening peak for each strain. Dashed boxes highlight the pre-dawn period, 3 h before lights-on. Sample sizes: 12:12 h LD CS (29), CS^{W} (42); 16:8 h LD CS (18), CS^{W} (16). **b**, Evening peak time for the flies in **a** is shown for each strain under 12:12 h (left) and 16:8 h LD (right). No significant differences were observed between strains (Wilcoxon test). **c**, Mean normalised pre-dawn activity for flies under 12:12 h LD (from **a**, within the indicated pre-dawn period). Asterisks indicate significant differences: ** = $P < 0.01$ (Wilcoxon test).

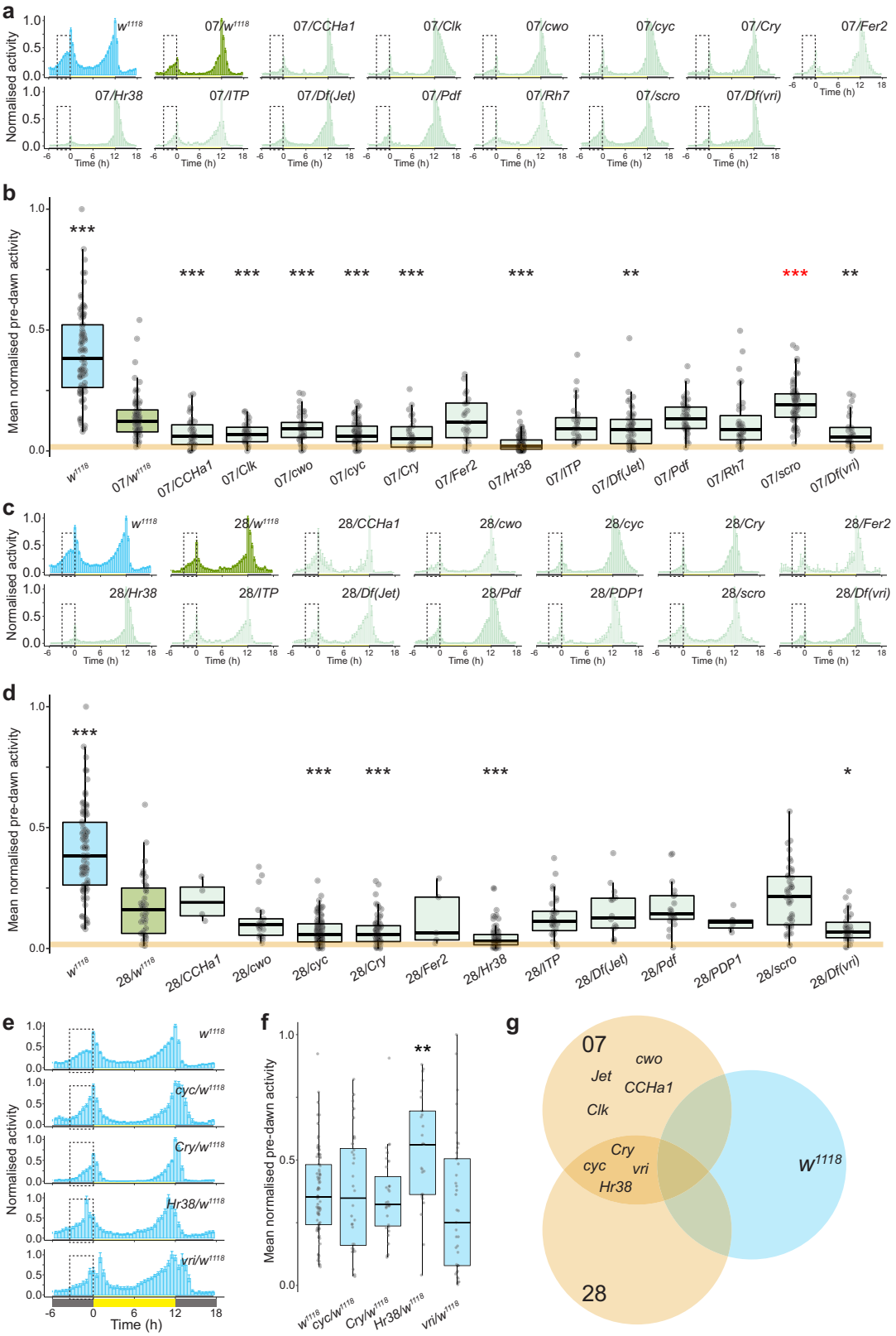

Extended Data Fig. 5 | See next page for caption.

Extended Data Fig. 5 | Screen results for the genetic basis of interspecific differences in morning activity. a, Mean normalised activity of the indicated genotypes under 12:12 h LD. Dashed boxes highlight the pre-dawn area used to quantify pre-dawn activity, 3 h before lights-on. Error bars represent SEM. Sample sizes: w^{1118} (78), 07/w^{1118} (69), 07/*CCHa1* (21), 07/*Clk* (34), 07/*cwo* (43), 07/*cyc* (43), 07/*Cry* (26), 07/*Fer* (18), 07/*Hr38* (87), 07/*ITP* (23), 07/*Jet* (49), 07/*Pdf* (42), 07/*Rh7* (33), 07/*scro* (58), 07/*vri* (28), 07 (40). **b**, Mean normalised pre-dawn activity for the genotypes in **a**. Asterisks indicate significant differences: ** = $P < 0.01$ and *** = $P < 0.001$ (Wilcoxon tests comparing each test hybrid to the control hybrid strain (07/w^{1118}) with Bonferroni correction). Red asterisks denote a significant increase in morning activity relative to control hybrids. The orange line marks the median pre-dawn activity of the *D. sechellia* parental strain (07). **c**, Mean normalised activity of the indicated genotypes under 12:12 h LD. Dashed boxes highlight the pre-dawn area used to quantify pre-dawn activity, 3 h before lights-on. Error bars represent SEM. Sample sizes: w^{1118} (78), 28/w^{1118} (22), 28/*CCHa1* (4), 28/*cwo* (20), 28/*cyc* (56), 28/*Cry* (66), 28/*Fer* (5), 28/*Hr38* (43), 28/*ITP* (25), 28/*Jet* (22), 28/*Pdf* (21), 28/*PDP1* (14), 28/*scro* (38), 28/*vri* (33), 28 (36). **d**, Mean normalised pre-dawn activity for the genotypes in **c**. Asterisks indicate significant differences: * = $P < 0.05$ and *** = $P < 0.001$ (Wilcoxon tests comparing each test hybrid to the control hybrid strain (28/w^{1118}) with Bonferroni correction). The orange line marks the median pre-dawn activity of the *D. sechellia* parental strain (28). **e**, Mean normalised activity of the indicated hemizygous *D. melanogaster* genotypes that displayed an effect in a hybrid background under 12:12 h LD. Dashed boxes highlight the pre-dawn area used to quantify pre-dawn activity. Plots depict average activity of the last 4 days of a 7-day recording period. Dashed boxes highlight the pre-dawn period, 3 h before lights-on. Error bars represent SEM. Sample sizes: w^{1118} (78), *cyc*/w^{1118} (31), *Cry*/w^{1118} (32), *Hr38*/w^{1118} (25), *vri*/w^{1118} (46). **f**, Mean normalised pre-dawn activity for the genotypes in **e**. Asterisks indicate significant differences: *Hr38* hemizygotes displayed a significant increase in morning peak activity compared to the control strain (w^{1118}). ** = $P < 0.01$ (Wilcoxon tests comparing each test hemizygote to the control strain (w^{1118}) with Bonferroni correction). **g**, Summary of the overlapping hits from each of the above genotypes. A priori, we considered the strongest candidates to display a reduction in morning peak activity in *Dsec*07 and *Dsec*28 hybrids, but not in w^{1118} hemizygotes. Four genes fulfilled these criteria: *cyc*, *Cry*, *Hr38* and *vri*.

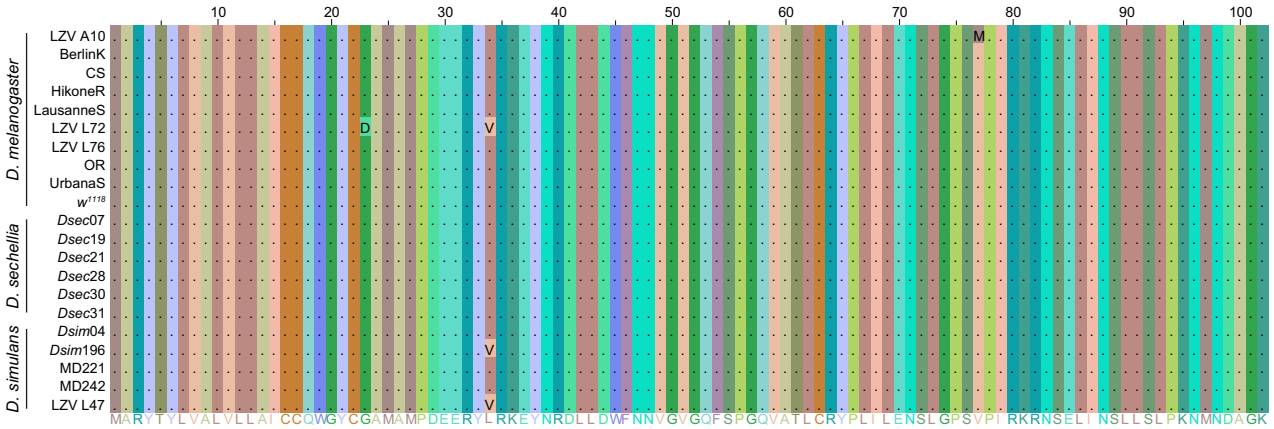

Extended Data Fig. 6 | The predicted Pdf peptide sequence is highly conserved between *D. melanogaster*, *D. sechellia* and *D. simulans*. Alignment of the predicted Pdf peptide sequence of 10 *D. melanogaster*, 6 *D. sechellia* and 5 *D. simulans* strains. The consensus sequence is displayed at the bottom. Amino acid residues were coloured by chemical similarity using JalView. Periods indicate conserved amino acid residues and letters indicate variable residues. No fixed differences are observed between species.

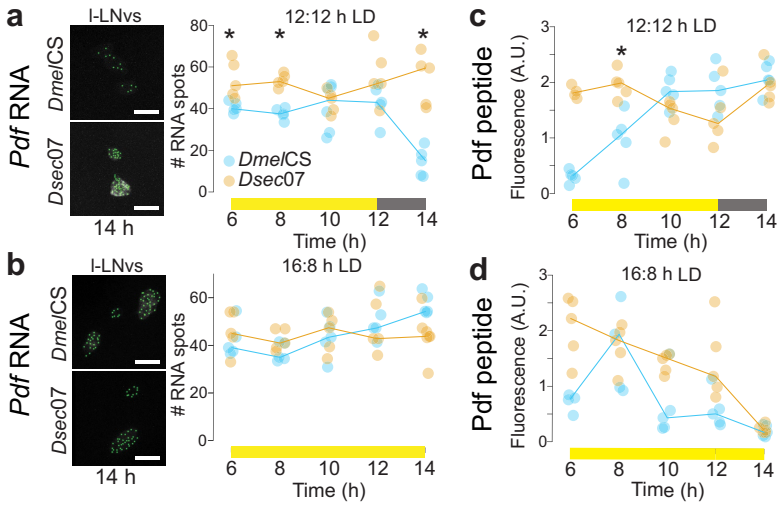

Extended Data Fig. 7 | Pdf expression in the l-LNvs of *D. melanogaster* and *D. sechellia* during the evening peak period. a,**b**, Left: representative images of *Pdf* smFISH in the l-LNv soma in *Dmel*CS and *Dsec*07 under 12:12 h LD (**a**) or 16:8 h LD (**b**) at one timepoint (14 h), with RNA spots (green) identified by RS-FISH. Right: quantifications of RNA spots at 5 timepoints spanning the evening activity peak period. **c**,**d**, Quantifications of Pdf signals in the l-LNv soma for *Dmel*CS and *Dsec*07 at 5 timepoints spanning the evening activity peak period under 12:12 h LD (**c**) and 16:8 h LD (**d**). For **a**-**d**, lines connect medians of each timepoint within genotypes. * = $P < 0.05$ (Pairwise Wilcoxon tests with Bonferroni correction).

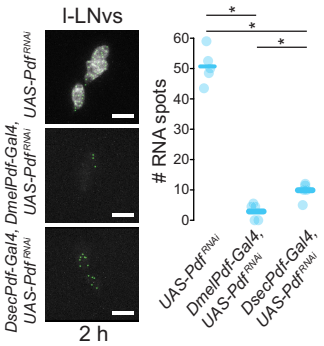

Extended Data Fig. 8 | Validation of differential *Pdf* transcript depletion by RNAi. Left: representative images of *Pdf* smFISH for one genetic control (*UAS-Pdf*^{RNAi}/+), *DmelPdf-Gal4/UAS-Pdf*^{RNAi} and *DsecPdf-Gal4/UAS-Pdf*^{RNAi} strains with RNA spots identified by RS-FISH. Right: quantifications of RNA spots. $n = 5$ for each genotype. * = $P < 0.05$ (Pairwise Wilcoxon tests with Bonferroni correction).

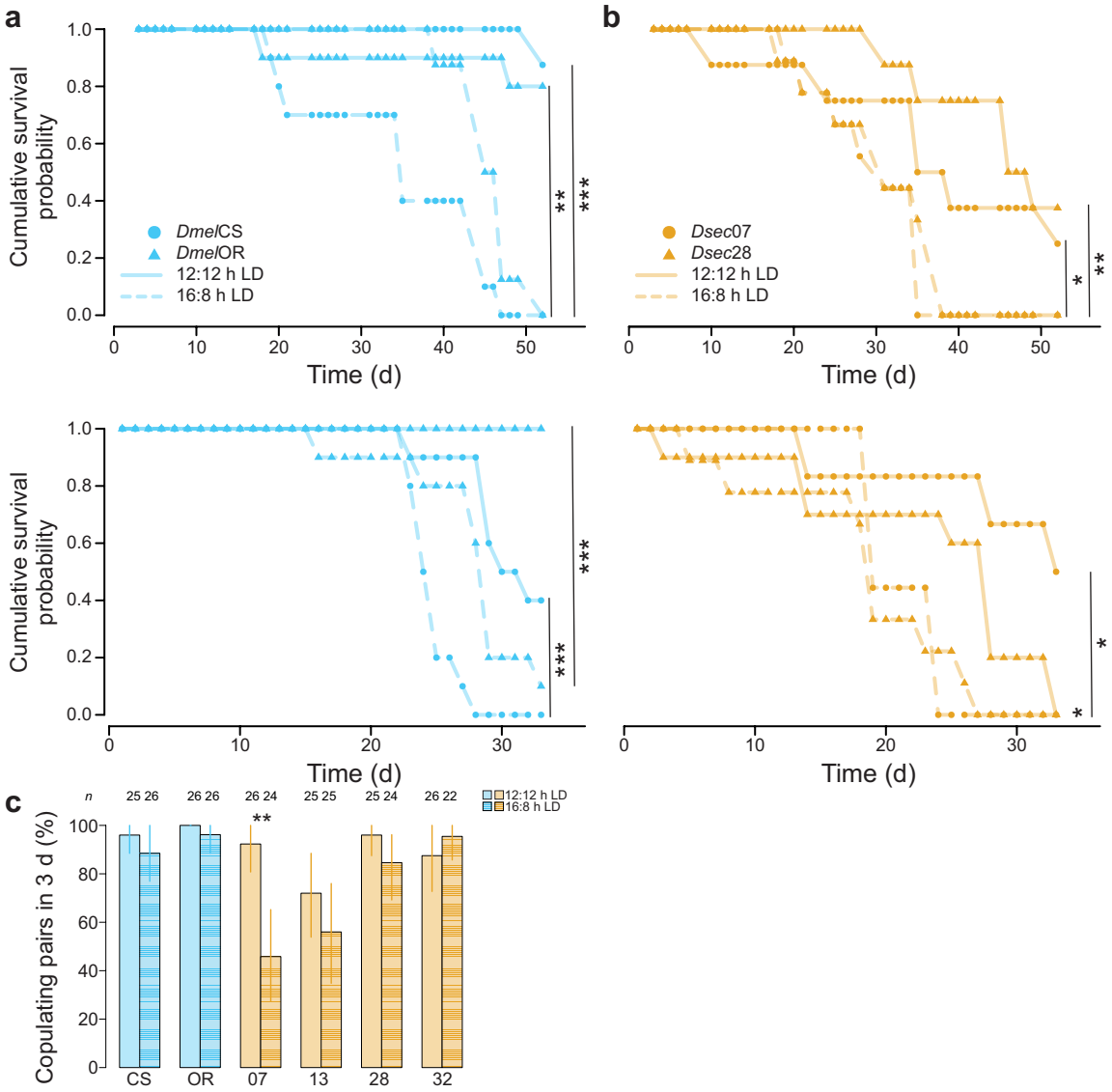

Extended Data Fig. 9 | Potential fitness effects of acclimating *D. melanogaster* and *D. sechellia* to 16:8 h LD. a, Two replicates (top and bottom) of the cumulative survival probability for *D. melanogaster* (*Dmel*CS and *Dmel*OR) maintained at 12:12 h LD or 16:8 h LD. No significant differences were observed between strains of the same species by photoperiod. **b**, Two replicates (top and bottom) of the cumulative survival probability for *D. sechellia* (*Dsec*07 and *Dsec*28) maintained at 12:12 h LD or 16:8 h LD. No significant differences were observed between strains of the same species by photoperiod. For **a**-**b**, asterisks indicate significant differences between photoperiod treatments of the same strain: * = $P < 0.05$, ** = $P < 0.01$ and *** = $P < 0.001$ (log-rank test). The top replicate in both panels is the same data presented in Fig. 5f (where it is pooled by species). **c**, Percent of copulating pairs observed for *D. melanogaster* (blue) and *D. sechellia* (orange) after 3 d for flies acclimated to 12:12 h LD (left) compared to 16:8 h LD (right). Error bars, representing 95% confidence intervals, were calculated using 1000 bootstraps. * = $P < 0.05$ and ** = $P < 0.01$ (Wilcoxon tests with Bonferroni correction for multiple comparisons).

nature portfolio

Corresponding author(s): Michael P. Shahandeh, Richard Benton

Last updated by author(s): Aug 16, 2024

Reporting Summary

Nature Portfolio wishes to improve the reproducibility of the work that we publish. This form provides structure for consistency and transparency in reporting. For further information on Nature Portfolio policies, see our Editorial Policies and the Editorial Policy Checklist.

Statistics

For all statistical analyses, confirm that the following items are present in the figure legend, table legend, main text, or Methods section.

n/a	Confirmed	
☐	☒	The exact sample size (*n*) for each experimental group/condition, given as a discrete number and unit of measurement
☐	☒	A statement on whether measurements were taken from distinct samples or whether the same sample was measured repeatedly
☐	☒	The statistical test(s) used AND whether they are one- or two-sided *Only common tests should be described solely by name; describe more complex techniques in the Methods section.*
☒	☐	A description of all covariates tested
☐	☒	A description of any assumptions or corrections, such as tests of normality and adjustment for multiple comparisons
☐	☒	A full description of the statistical parameters including central tendency (e.g. means) or other basic estimates (e.g. regression coefficient) AND variation (e.g. standard deviation) or associated estimates of uncertainty (e.g. confidence intervals)
☐	☒	For null hypothesis testing, the test statistic (e.g. *F*, *t*, *r*) with confidence intervals, effect sizes, degrees of freedom and *P* value noted *Give P values as exact values whenever suitable.*
☒	☐	For Bayesian analysis, information on the choice of priors and Markov chain Monte Carlo settings
☒	☐	For hierarchical and complex designs, identification of the appropriate level for tests and full reporting of outcomes
☐	☒	Estimates of effect sizes (e.g. Cohen's *d*, Pearson's *r*), indicating how they were calculated

Our web collection on statistics for biologists contains articles on many of the points above.

Software and code

Policy information about availability of computer code

Data collection	Confocal images were obtained using the Zeiss microscopy ZEN 2.3 SP1 software. Drosophila Activity Monitor data were collected using the DAM System software, version 311X.
Data analysis	All image analysis was performed in Fiji running v2.9.0 of ImageJ. RNA spots were detected using the RS-FISH macro, and Scholl analysis was performed using the neuroanatomy plug-in. Sequences were analyzed and visualised using SnapGene (www.snapgene.com) running MUSCLE (v3.8.1551), and Jalview (v2.11.2), and using the R package Phangorn (v2.11.2). Sequence alignments were perfomed using Samtools (v1.19.2), and tests of neutrality were performed using the DNA sequence polymorphism software (v6). Drosophila Activity Monitor data were analysed using Rethomics in R (v3.6.3). All R code used for data analysis are available at: github.com/mshahandeh/circ_plasticity.

For manuscripts utilizing custom algorithms or software that are central to the research but not yet described in published literature, software must be made available to editors and reviewers. We strongly encourage code deposition in a community repository (e.g. GitHub). See the Nature Portfolio guidelines for submitting code & software for further information.

Data

Policy information about availability of data

All manuscripts must include a data availability statement. This statement should provide the following information, where applicable:

- Accession codes, unique identifiers, or web links for publicly available datasets
- A description of any restrictions on data availability
- For clinical datasets or third party data, please ensure that the statement adheres to our policy

All data generated for this study are available in the Dryad digital repository (doi:10.5061/dryad.vq83bk42z).
We additionally used D. melanogaster SNV data from PMID 26547394 (data available at Dryad doi:10.5061/dryad.7440s)
We used sequences of D. sechellia from PMID 29684059 (available from SRA:SRP113415). To align these sequences, we used the D. sechellia reference genome (ASM438219v2).

Research involving human participants, their data, or biological material

Policy information about studies with human participants or human data. See also policy information about sex, gender (identity/presentation), and sexual orientation and race, ethnicity and racism.

Reporting on sex and gender	N/A
Reporting on race, ethnicity, or other socially relevant groupings	N/A
Population characteristics	N/A
Recruitment	N/A
Ethics oversight	N/A

Note that full information on the approval of the study protocol must also be provided in the manuscript.

Field-specific reporting

Please select the one below that is the best fit for your research. If you are not sure, read the appropriate sections before making your selection.

☒ Life sciences ☐ Behavioural & social sciences ☐ Ecological, evolutionary & environmental sciences

For a reference copy of the document with all sections, see nature.com/documents/nr-reporting-summary-flat.pdf

Life sciences study design

All studies must disclose on these points even when the disclosure is negative.

Sample size	No statistical methods were used to predetermine sample size. For behavioural experiments, we aimed for a sample size of 25-30 individuals, as significant differences were easily detected at these sizes. In the case of our hybrid screen, where hybrid flies were harder to make, we aimed for 15 individuals per strain but due to the strong reproductive isolation between species, some genotypes were difficult to cross to D. sechellia, resulting in a lower sample size. For image analyses, we obtained images from 5 brains from each strain per treatment because this allowed for parallel processing of multiple genotypes and time points. Additionally, quantifications of these stainings were largely consistent and significant differences were apparent at this sample size.
Data exclusions	No data were excluded.
Replication	All behavioural experiments were collected over at least two technical replicates with corresponding controls to ensure reproducibility, with the exception of those shown in Fig. 1c, where we replicated only two photoperiod treatments: 12:12 h LD and 16:8 h LD, because we continued the use of these specific photoperiods throughout the work. All brain dissections and stainings for a given experiment were performed in parallel to ensure comparability between time points and fixed microscope settings were used within each experiment. Two time-points of each histological experiments (Pdf smFISH, Pdf immunofluorescence, and Scholl analysis of s-LNv axonal projections) were replicated once in order to ensure the overall patterns of expression were the same.
Randomization	We did not randomise within experiments, and instead ran all genotypes in parallel for all experiments, except for the hybrid screening, where we measured the behaviour of hybrids as and when crosses produced offspring, with at least one replicate run in parallel with corresponding controls (data collection for hybrid screening took >2 years).
Blinding	Quantifications for stainings and collection of behavioural data were performed blind to treatment.

Reporting for specific materials, systems and methods

We require information from authors about some types of materials, experimental systems and methods used in many studies. Here, indicate whether each material, system or method listed is relevant to your study. If you are not sure if a list item applies to your research, read the appropriate section before selecting a response.

Materials & experimental systems

n/a	Involved in the study
☐	☒ Antibodies
☒	☐ Eukaryotic cell lines
☒	☐ Palaeontology and archaeology
☐	☒ Animals and other organisms
☒	☐ Clinical data
☒	☐ Dual use research of concern
☒	☐ Plants

Methods

n/a	Involved in the study
☒	☐ ChIP-seq
☒	☐ Flow cytometry
☒	☐ MRI-based neuroimaging

Antibodies

Antibodies used	All antibodies used are described in Supplementary Table 2.
Validation	All antibodies were previously validated: - mouse anti-Pdf, obtained from DSHB with confirmed species reactivity in Drosophila for IHC-IF (https://dshb.biology.uiowa.edu/PDF-C7) - rat anti-Cadherin-N, obtained from DSHB with confirmed species reactivity in Drosophila for IHC-IF (https://dshb.biology.uiowa.edu/DN-Ex-8) - rabbit anti-GFP, Molecular Probes AB_221570; this is a fully-validated commercial antibody

Animals and other research organisms

Policy information about studies involving animals; ARRIVE guidelines recommended for reporting animal research, and Sex and Gender in Research

Laboratory animals	All fly strains used are described in Supplementary Table 1. All fly strains were domesticated and have been reared in common laboratory conditions for 20+ years, with the exception of the MD and LZV strains, which were collected and domesticated in ~2014 (PMID 24920013). For all experiments, flies were 3-5 days old at the start of the experiment.
Wild animals	No wild animals were used in this study.
Reporting on sex	As is standard in the Drosophila circadian field, we only used males in most of the experiments of this study because they do not reproduce within the long-term behavioural assay. Males were identified by the presence of the male genital arch under a stereo-microscope. However, we verified that the key species-specific behaviours described in males were also observed in females (Extended Data Fig. 1c-d).
Field-collected samples	No field-collected samples were used in this study.
Ethics oversight	No ethical approval or guidance was required for this study, as we used exclusively invertebrate animals.

Note that full information on the approval of the study protocol must also be provided in the manuscript.